SBIR Phase I Final Report

Sheet Electron Probe for Beam Tomography

by

Muons, Inc.

12/07/2021

DOE award number: SBIR Project DE-SC0021581
Name of Recipient: Muons, Inc.

Project Title: SHEET ELECTRON PROBE FOR BEAM TOMOGRAPHY

Name of PI: Dr. Vadim Dudnikov

Date of Report: December 7, 2021
Period of Project: From 02/22/2021 through 11/21/2021

ABSTRACT

Advanced beam diagnostics are essential for high performance accelerator beam production and for reliable accelerator operation. It is important to have noninvasive diagnostics which can be used continuously with intense beams of accelerated particles. Noninvasive determination of accelerated particle distributions is the most difficult task of bunch diagnostics. A pencil electron beam probe was successfully developed and used at the ORNL SNS for the determination of accelerated particle density distributions. However, the apparatus used for this is large and complex, which complicates the broad use of this technique for tomography of accelerated bunches.

In the novel device to be developed in this project, a simple, strip cathode provides a sheet beam probe for tomography instead of a scanning pencil beam that was used in the previous electron probe bunch profile monitor. The apparatus with the strip cathode is smaller, has simpler design and less expensive manufacturing, has better magnetic shielding, has higher sensitivity, higher resolution, has better accuracy of measurement, and better time resolution. With this device it is possible to develop almost ideal tomography diagnostics of bunches in linear accelerators and in circular accelerators and storage rings.

In this Phase I SBIR project, the design of an electron probe with a strip cathode was optimized and plans for its construction prepared. Computer codes for simulation of strip electron beam deflection by ultra-relativistic proton bunches were also developed. Discussions were initiated with groups at BNL (RHIC and BLIP), FRIB, FNAL (PIP-II) and ORNL for first beam tests of the sheet e beam tomography system at the end of the Phase II project. The most advantageous choice and an appropriate agreement will be made in the first year of the Phase II project. We anticipate that the tomography system developed in this project will be important for the DOE NP Electron Ion Collider as well as other accelerator projects in the US and around the world.

Table of Contents - Phase I Final Report

SHEET ELECTRON PROBE FOR BEAM TOMOGRAPHY

Table of Contents

Project Description

Introduction -

Advanced beam diagnostics are essential for high performance accelerator beam production and for reliable accelerator operation. It is important to have noninvasive diagnostics which can be used continuously with intense beams of accelerated particles. Noninvasive determination of accelerated particle distributions is the most difficult task of bunch diagnostics. Recently, a pencil electron beam probe was successfully used for determination of accelerated particle density distributions. However, the apparatus used for this is large and complex, which complicates the broad use of this technique for tomography of accelerated bunches.

In the novel device to be developed in this project, a simple strip cathode provides a sheet beam probe for tomography instead of a scanning pencil beam that was used in previous electron probe bunch profile monitors. The apparatus with the strip cathode is smaller, has simpler design and less expensive manufacturing, has better magnetic shielding, has higher sensitivity and higher resolution, has better accuracy of measurement, and has better time resolution. With this device it is possible to develop almost ideal tomography diagnostics of bunches in linear accelerators and in circular accelerators and storage rings.

The development of a compact, reliable, and robust source of the sheet electron probe is vital for the successful development of the full tomography system. An engineering design of a sheet electron probe system with a strip cathode and computer simulations was developed in Phase I. In Phase II the full prototype tomography system with improved hardware and software will be developed and tested in proton or ion beams.

The proposed electron probe tomography system with the strip cathode should be the most advanced system for detailed diagnostics of accelerated beams. It can be used in all advanced accelerators and storage rings such as SNS, main injector FNAL, RHIC, LHC, ISIS, KEK and many others. Serial production of these diagnostics will lower costs and improve operation of these facilities and some new multi-billion dollar facilities that are planned.

Beam profile determination for high intensity accelerators implies the use of non-destructive methods. The basic physics and recent technical realizations of important non-intercepting profile diagnostics are summarized in Ref. [1]. Ionization Profile Monitors (IPM) and Beam Induced Fluorescence Monitors (BIFM), developed and first used with intense proton beams by Dudnikov [2,3,4], are now routinely used in all proton and ion accelerators. Recent developments of IPM are presented in [1,5].

Transverse electron beam scanners (TEBS) were realized recently for use in the SNS storage ring by Aleksandrov et al. [4,6]. Laser beam scanners are used at H^- Linacs, Optical Transition Radiation screens, and Synchrotron Radiation Monitors for relativistic beams. Non-destructive transverse profile measurements are preferred not only for single-path diagnostics at different locations in a transfer line, but also to enable time resolved observations of a stored beam within a synchrotron. A more practical, however essential, reason for minimally invasive diagnostics is the large beam power available at modern hadron accelerators, which excludes the usage of intercepting methods like scintillation screens, SEM-grids or wire scanners due to the risk of melting when irradiated by the total beam intensity.

Various methods are realized to determine the profile properties of typical widths σ = 0.1 to 10 mm of not necessarily Gaussian shapes. In most synchrotrons and storage rings the transverse profile of the circulating beam is monitored via detecting the ionization products from the collision of hadrons with residual gas by an Ionization Profile Monitor (IPM). These are relatively complex and expensive: the IPM system for the Tevatron cost ~$0.3 M$.

Technical Approach

Description of SNS Pencil electron Beam Profile Monitor

To appreciate the advantages of the proposed sheet beam probe system, it is useful to describe the present SNS system and its limitations. In the SNS system the transverse profile is reconstructed from the deflection of electrons crossing the ion beam and being influenced by the beam's space charge, as schematically shown in Fig. 1 from [1]. A pencil electron beam probe, similar to a TV tube electron beam, is formed by an electron gun and scanned through the proton beam by the electric field of a deflector as in an oscilloscope tube. The position of the scanning e beam probe after crossing the proton beam is visualized by a fluorescent screen and its image is captured by a CCD camera for further processing.

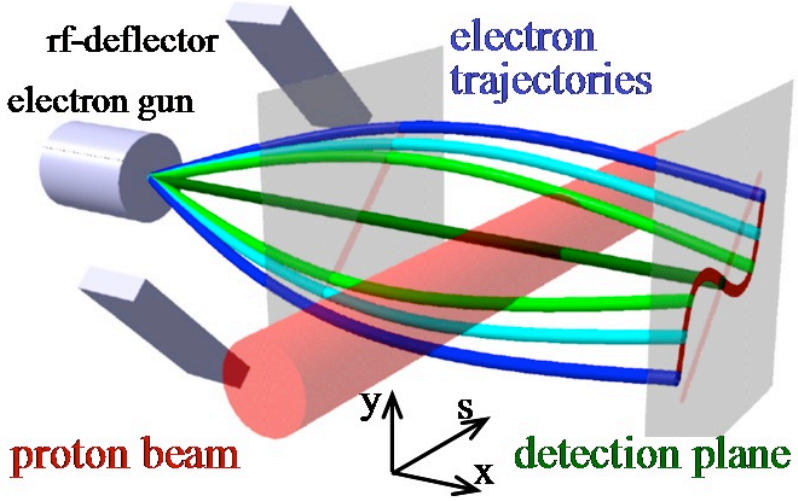

Figure 1: Schematic of a pencil electron beam scanner for the vertical beam profile (from [1]).

Assuming the electron beam has a much smaller diameter than the ion beam and the scan duration is much shorter than the ion bunch passage, the space charge field can be treated as constant. The deflection angle is maximal at the beam edge and decreases during the scan towards the beam center; no deflection occurs when passing the center. The electron trace in the detector plane is recorded. The diagonal deflection ensures that the profile information is extracted from the derivative of this trace with respect to the beam direction. This method was considered for high energy synchrotrons [4] and recently commissioned at the SNS [5]. Using a scanning ion beam instead of electrons, the method was analyzed and tested at CERN [7]. The deflection of the probe beam due to the electric field of the bunches is calculated in Ref. [8]. The corresponding mathematical formalism for profile reconstruction is given in Ref. [9]. The setup at the SNS-Ring [5] shown in Fig. 2 consists of an electron gun (1) providing a pencil electron beam of up to 75 keV and 5 mA for 1 μs pulses at 5 Hz repetition rate. The beam passes an electric deflector (2) for a diagonal sweep of 20 ns duration and two quadrupoles (4)

to enlarge the spatial range and parallelize the beam during scanning. After crossing the ion beam (5), where the deflection occurs, the electrons are visualized by a phosphor screen (6) and recorded with a camera. To achieve a reasonable deflection, the electron beam energy must be matched to the ion beam current. The advantage of the possibility of sliced profile measurements with high time resolution is given by the short sweep duration of only 20 ns. The transverse profile is derived from the angle of deflection of the electron beam according to the following formula, see also [5]:

$$\frac{d\theta}{dx} = \int_L \frac{e}{mv^2} \cdot \frac{\delta(x,y)}{\varepsilon_0} dy$$

where *e, m* are the electron charge and mass, respectively, with the velocity v, $\delta(x,y)$ is the ion beam density distribution, and θ is the electron beam deflection angle. In other words, the derivative of the deflection angle as a function of impact parameter is proportional to the Y-integrated profile of the transverse beam charge distribution QL. This happens to be precisely the same information as one obtains from a probe wire ("flying wire") which is passed perpendicular to the beam in the Y-direction (that of the probe electron) through the X-point corresponding to that electron's impact parameter b. This assumes that the path of the electrons is approximately straight, the net energy change to the electrons by the proton beam is close to zero, and the effect of the ion magnetic field can be neglected.

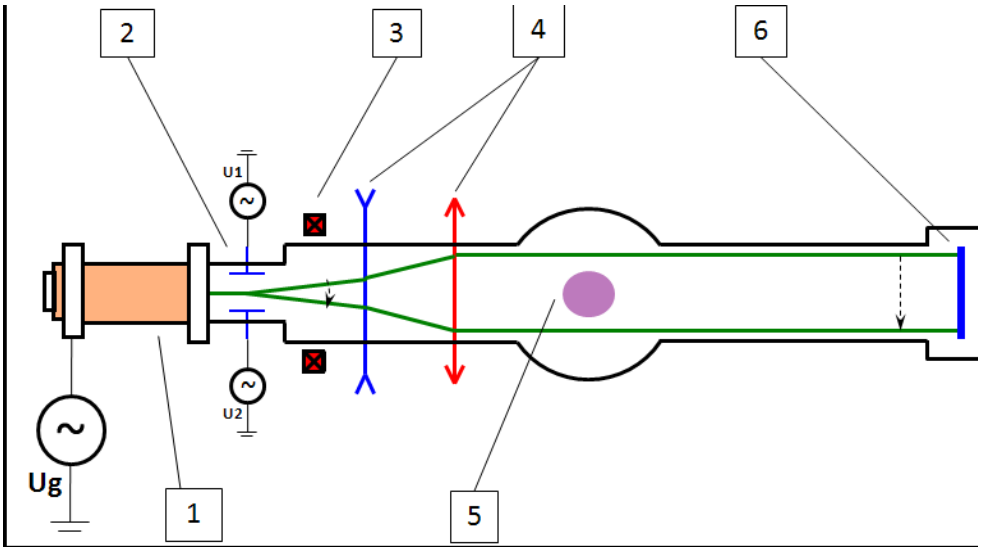

Fig. 2: Diagram of the SNS electron scanner from Ref. [5], where 1 is the electron gun, 2 is the deflection scan system, 3 are the dipole correctors, 4 indicates the quadrupole magnets, 5 is the vacuum chamber of the proton beam, and 6 is the luminescent screen.

The first quadrupole extends the range of the deflection while the second quadrupole focuses the electron beam such that the electron beam is parallel. The electron gun is pulsed once a second but faster rep rates of up to 5 Hz are possible. Vision CMOS cameras acquire the images from the fluorescent screens. Because the scanners are in a straight section of the ring, the radiation levels are low enough to not damage the cameras. A single PXI-based computer running LabVIEW controls the cameras, timing, pulse generators and power supplies of the electron scanner. A significant part of the scanner is used for extension of the scanning e beam and bulky quadrupole magnets complicate the magnetic shielding of this version of the scanner. For these reasons, the electron beam profile monitor (EBPM) with electron beam deflection of a pencil e-beam is very long, bulky, and complex. A more

practical e-beam profile monitor suitable for proton/ion beam tomography can be developed using a strip cathode to form a sheet beam as described below.

SNS Pencil Electron Beam Scanner Software

The software for the electron scanner consists of four parts:

1) Control software that controls the electron scanner hardware, including the timing.
2) Simulation software that simulates the projection of the electrons and creates test images for the analysis software.
3) Imaging software that acquires the image of the projected electrons and analyzes the curve to determine the transverse profile.
4) Scan software that manages the Control software and the Imaging software to perform multiple acquisitions and produces 3-dimensional images of the beam bunch, e.g. a longitudinally integrated profile.

Both the Imaging and the Scan software interface to EPICS so that the physics applications on the consoles can read out the results. An example of simulation results is shown in Fig. 3.

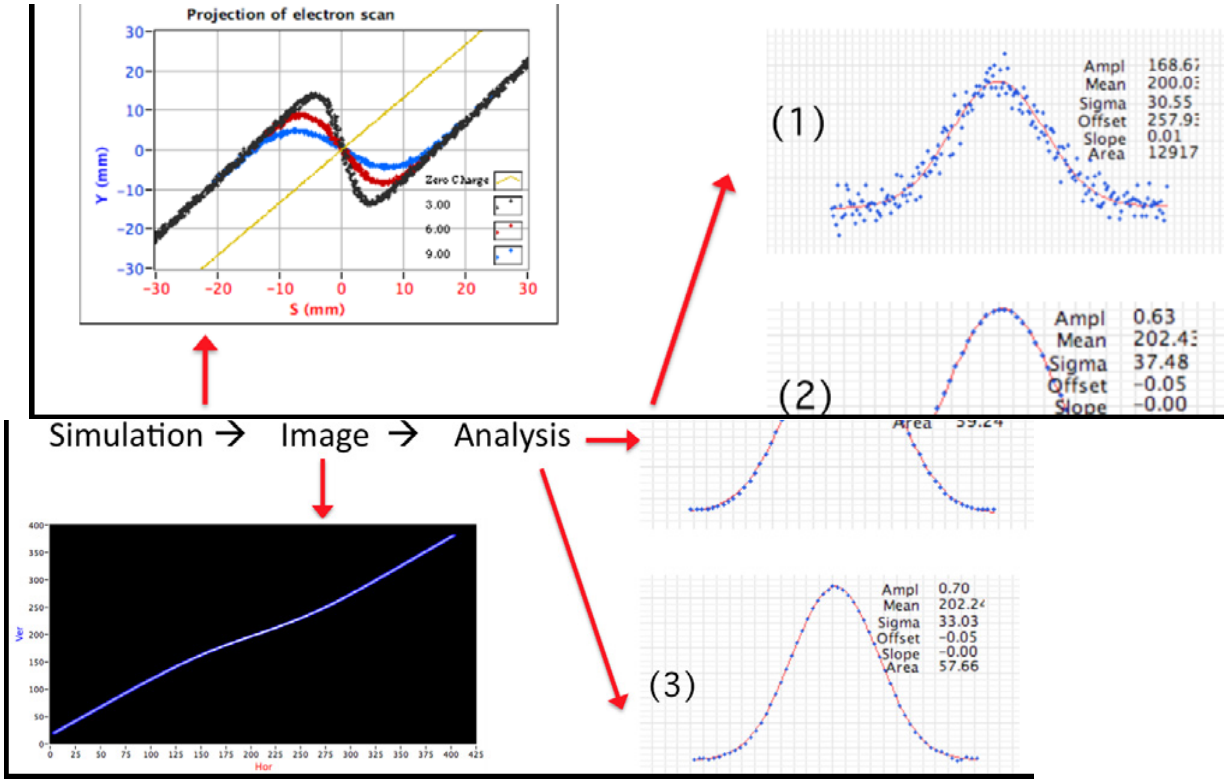

Fig. 3: Simulated Electron projections, generated images, and different profile analysis fits

The analysis has to take the derivative, dy/dx, of the curve to determine the profile. Because taking the derivative of data, especially pixel data from the camera, can provide noisy results, different analysis methods were tested ahead of commissioning using the simulation software. These methods were: (1) find the peak in each column of pixels to find an (x, y) pair and take the derivative of all (x, y) pairs, (2) find the peak of a Gaussian fitted to each column of pixels to get (x, y, z) pair information plus (z

peak intensity(z), then fit these pairs with a spline and take the derivative of the fit, or (3) fit a spline to all pixels weighted by intensity, and take the derivative of the fitted spline, see Fig. 3. The smoothing provided by the spline and Gaussian fit in method (2) most effectively mitigated the image noise problem and thus yielded the most reliable results. The spline fitting can find a profile even if there are gaps in the electron curve due to low electron density.

An example of the horizontal projected electron curve is shown in Fig. 4. The bright spot on the right consists of electrons that are outside the 20 ns deflection scan waveform but still are accelerated by the 1usec long accelerating pulse.

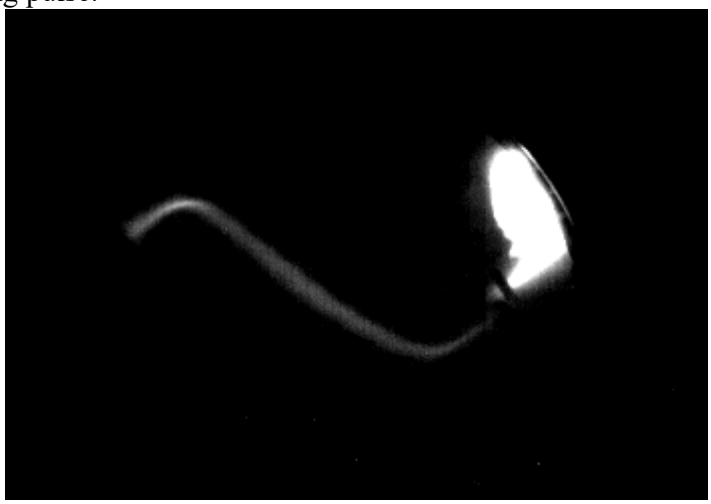

Figure 4: Image of the electron curve. The e beam scan is 60 mm and the beam energy is 65 keV.

Because the length of the scan is short, 20 ns, compared to the bunch length of 600 ns, we can perform scans at different locations within the bunch. By performing scans at regular intervals throughout entire bunch length, we can create 3-dimensional plots of the bunch, as shown in Fig. 5. A double peak in the longitudinal direction is confirmed by the Ring Current Monitor waveform.

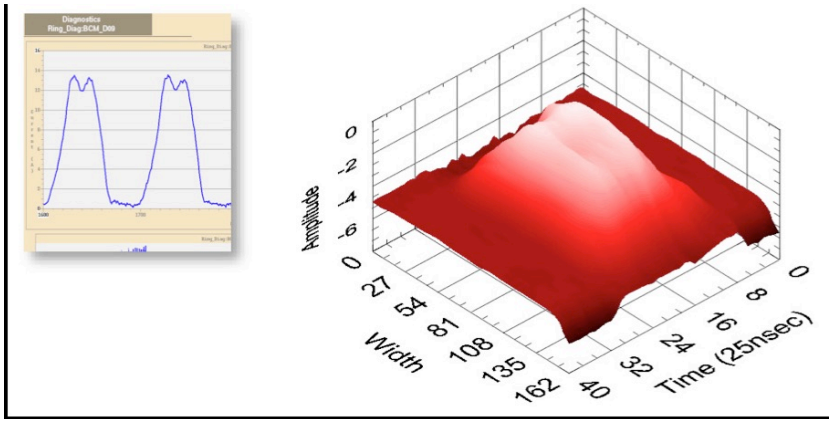

Figure 5: Shown on right is the 3-D profile for a 4 μC bunch in the accumulator ring.

The width axis represents the transverse axis of the beam and is given in pixels with 0.3 mm per pixel. The time axis represents the longitudinal axis of the beam and is given in 25 ns per count. Shown on the left is the longitudinal profile as given by a ring beam current monitor.

Advanced Sheet Electron Probe Beam Profile Monitor

The advanced sheet electron probe beam profile monitor (SEPBPM) with the proposed strip cathode is shown in Fig. 6. The slice (4) of the sheet electron probe is formed by the strip cathode (1) with extractor (2) and accelerating electrode (3). The short slice (4) is formed by pulsed volage applied to extraction electrode (2). After deflection by the electric field of the proton bunch (5), the electrons of the slice hit the luminescent screen (6) and recorded by a fast CCD camera for further processing by corresponding software discussed above.

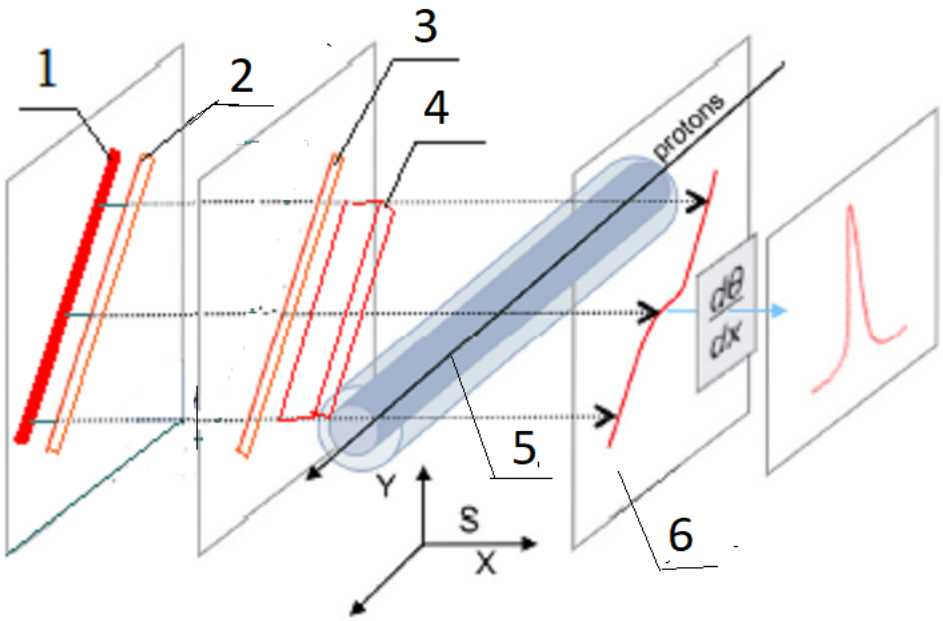

Fig. 6. Electron probe beam profile monitor with a strip cathode. Element 1 is the strip cathode, 2 is the extraction electrode; 3 is the accelerating electrode, 4 is the slice of the sheet electron beam probe, 5 is the ion bunch, 6 is the luminescent screen.

This version of the SEPBPM is smaller, easier to fabricate, operate and employ magnetic shielding. Several similar systems can be integrated for production of the tomographic 3-D image of proton bunches. The proposed tomographic system is more compact, easier to operate and less expensive than residual gas ionization profile monitors (IPM) discussed above. A simplified diagram of a SEPBPM is shown in Fig. 7

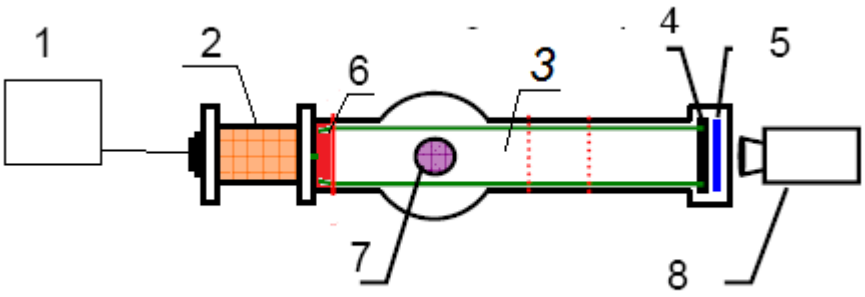

Fig. 7. A simplified diagram of SEPBPM. Element 1 is the high voltage pulser; 2 is the high voltage insulator of the electron gun, 3 is the sheet slice of the electron probe, 4 is the MCP; 5 is the luminescent

screen, 6 is the sheet electron source (made of items 1 through 5 of Fig. 6), 7 is the proton/ion bunch; 8 is the CCD camera.

A slice of the sheet electron beam (3) is formed by the sheet electron source (6) and crosses the bunch (7). Sheet electrons are deflected by electric and magnetic fields of the bunch (7). This deflection is sensed by the position of the electron images on the luminescent screen (5) and recorded by the CCD camera (8). Electron multiplication with a microchannel plate (MCP) (4) can be used for synchronization and for brightness amplification. A high voltage (~50 kV) power supply (1) is used for electron beam acceleration (pulsed extraction. An electron source cathode (1) is supported by a high voltage insulator (2). An isometric view of diagnostic system is shown in Fig. 8 below.

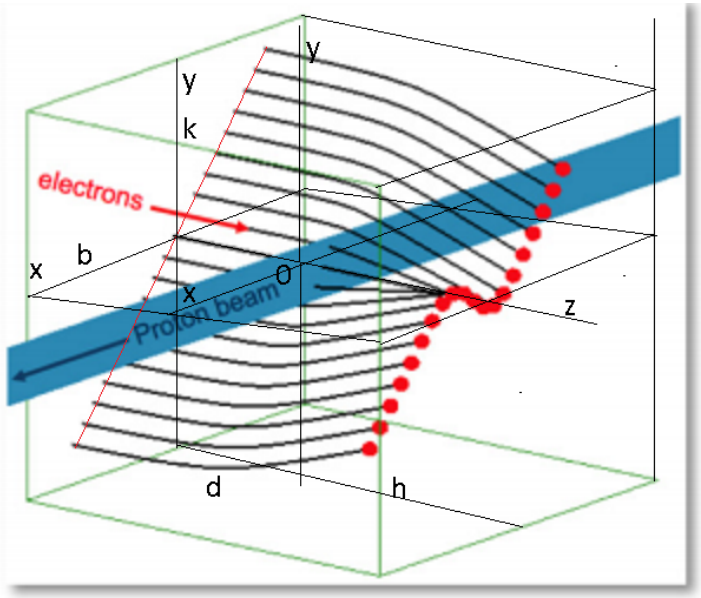

Fig. 8: Isometric view of the strip e-beam profile monitor with a slice of the sheet electron probe.

We need to find the solution for deflection of electrons of the slice of the electron probe of the sheet electron probe by space charge of the proton beam in the box with dimension +-b along x axis, +-k in y direction and d +h in z direction. The planes x= +-b, y=+-k, z=k and h are conductive and components of the electric field equal zero.

The proton bunch charge distribution is given by the formula:

$P(x,y,z)=Q\ (\exp -x^2/a^2-y^2/b^2-z^2/c^2)$

The cathode is located in the xy plane at a distance d from center of the proton beam on the line y=x and has length L. Electrons start from the cathode with velocity v parallel to the z axis z, are deflected by the electric field of space charge, and accepted by the screen at the xy plane at a distance h from center of the proton beam.

Phase I Work Plan

The Phase I Work Plan consisted of the following tasks:

1. Develop computer codes for simulation of strip electron beam deflection by ultra-relativistic proton bunches
2. Optimize deflection system using computer simulations
3. Design and simulate prototypes of the electron probe source with a strip cathode
4. Develop a project of versions of thermionic cathodes
5. Design electron gun with strip cathode
6. Use PBGUN computer simulations to optimize electron beam formation
7. Prepare the mechanical design of the electron gun
8. Optimize beam formation

Degree to which Phase I has Demonstrated Technical Feasibility

During Phase I, computer codes for the simulation of the probe electron beam deflection by an ion bunch were prepared. The development of strip the cathode electron gun for sheet electron beam formation was prepared. The development of a luminescent screen with MCP enhancement was prepared.

The performance goals and schedule of the Phase I project were:

3 months - Develop computer codes for simulation of strip electron beam deflection by ultra-relativistic proton bunches
Optimize deflection system using computer simulations
6 months - Design and simulate prototypes of the electron probe source with a strip cathode
Design electron gun with strip cathode
Use PBGUN computer simulations to optimize electron beam formation
9 months - Phase II proposal prepared

All elements of this schedule were accomplished during the Phase I project.

Results of sheet electron beam tomography development in Phase I

Design of the strip cathode electron gun.

For generation of a Sheet electron Probe Beam it is possible to use the electron gun shown in Fig. 9. The Iridium Cerium (IrCe) alloy was verified at SuperKEKB as a photocathode material with excellent stability and longevity [10].

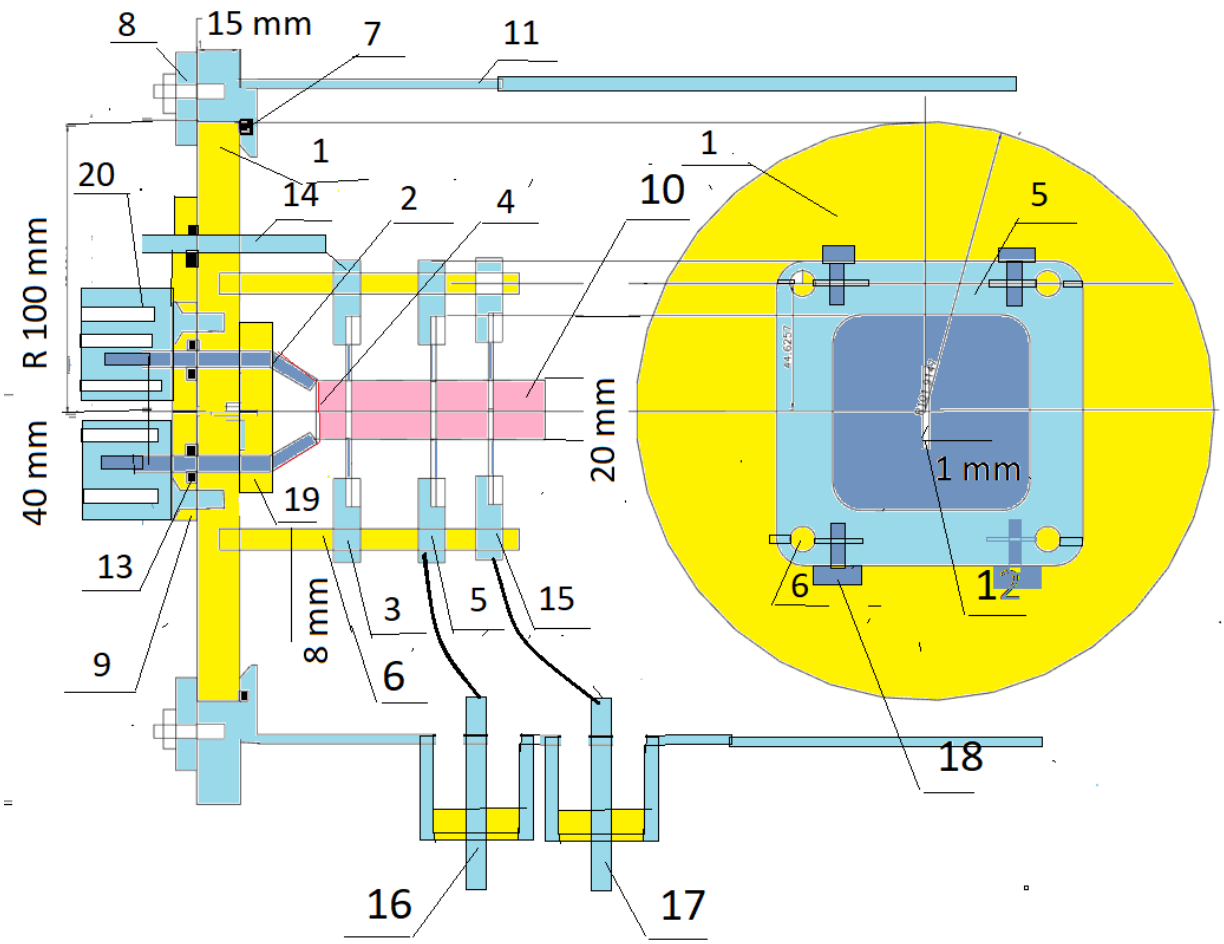

Fig. 9. Design of electron gun for production of Sheet electron Probe Beam.
1-ceramic disc (MACOR), 2-current leads (material stainless steel), 3- extractor electrode, 4- IrCe emitter of electrons 0.1x2x20 mm, 5-accelerating electrode, 6-ceramic support roads, 7-flange (material stainless steel), 8-compression flange, 9-compression ceramic, 10-sheet electron Probe Beam, 11-vacuum chamber (material stainless steel)., 12-emission slit, 13-o-rings, viton, 14-lead for extraction electrode, 15-focusing electrode, 16-feedthrough for accelerating electrode, 17-feedthrough for focusing electrode, 18-compressing bolts, 19-compression plates, 20-radiators.

The electron gun consists of a machinable ceramic disc with diameter of 20 cm and thickness of 15 mm (https://ceramics.ferrotec.com/products/machinable/), two current leads 2 (material stainless steel), diameter of 4 mm, for emitter heating, IrCe emitter of electron 4 of 2x20 mm, with curvature radius 5 mm, welded to current leads 2 by spot welding, extractor electrode 3 with aperture 1x20 mm, accelerating electrode 5 with aperture 1x20 mm, focusing electrode 15 with

aperture 1x20 mm, four ceramic support rods 6 with diameter 5-6 mm , Stainless steel flange 7, compression flange 8, compression disc (material KEEP polyetheretherketone polymer)) 9 with places for O- rings 13. Sheet electron Probe Beam 10 is emitted by IrCe emitter 4 and accelerated by extraction electrode 3 and accelerating electrode 5. High voltage -up to 100 kV is applied to emitter. Pulsed extraction voltage ~ 3 kV is applied to the extraction electrode by lead 14 and extract sheet electron beam. The electron beam passes through the proton bunch, is deflected by its electric and magnetic fields, and registered by the luminescent screen with the pulsed microchannel plate. The feedthroughs are sealed for vacuum by O-rings 13.

The lifetime of the IrCe cathode is up to 40,000 hours while generating current density of 15-17 A/cm^2 [10]. The drawing of the current leads is presented in Fig. 10. Voltages to accelerating electrode 5 is conducted by insulated lead 16. Voltages to focusing electrode 15 is conducted by insulated lead 17. Electrodes are compressed to ceramic support rods 6 by compressing bolts 18.

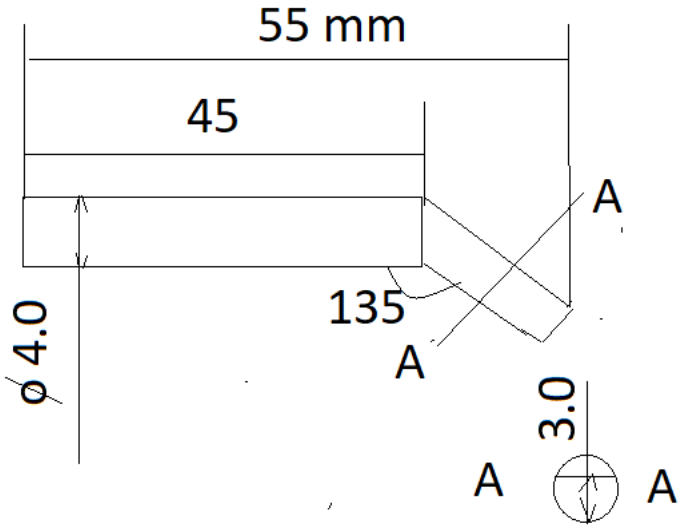

Fig. 10. Drawing of current lead (material stainless steel).

Stefan-Boltzmann
σT^4 is 21.8 W/cm^2 =5.67*10^{-8} (watt/m^{2}K^4)*10^{-4}(m^2/cm^2)*1400^4

Area of emitter = 0.01*2*2+0.2*2*2=0.88 cm^2
Cross section of emitter 0.01 x0.2 cm^2, Radiation Area of emitter 0.88 cm^2

Power 21.8x0.8=17.5 W

Radiated 17.5x0.4=7 W

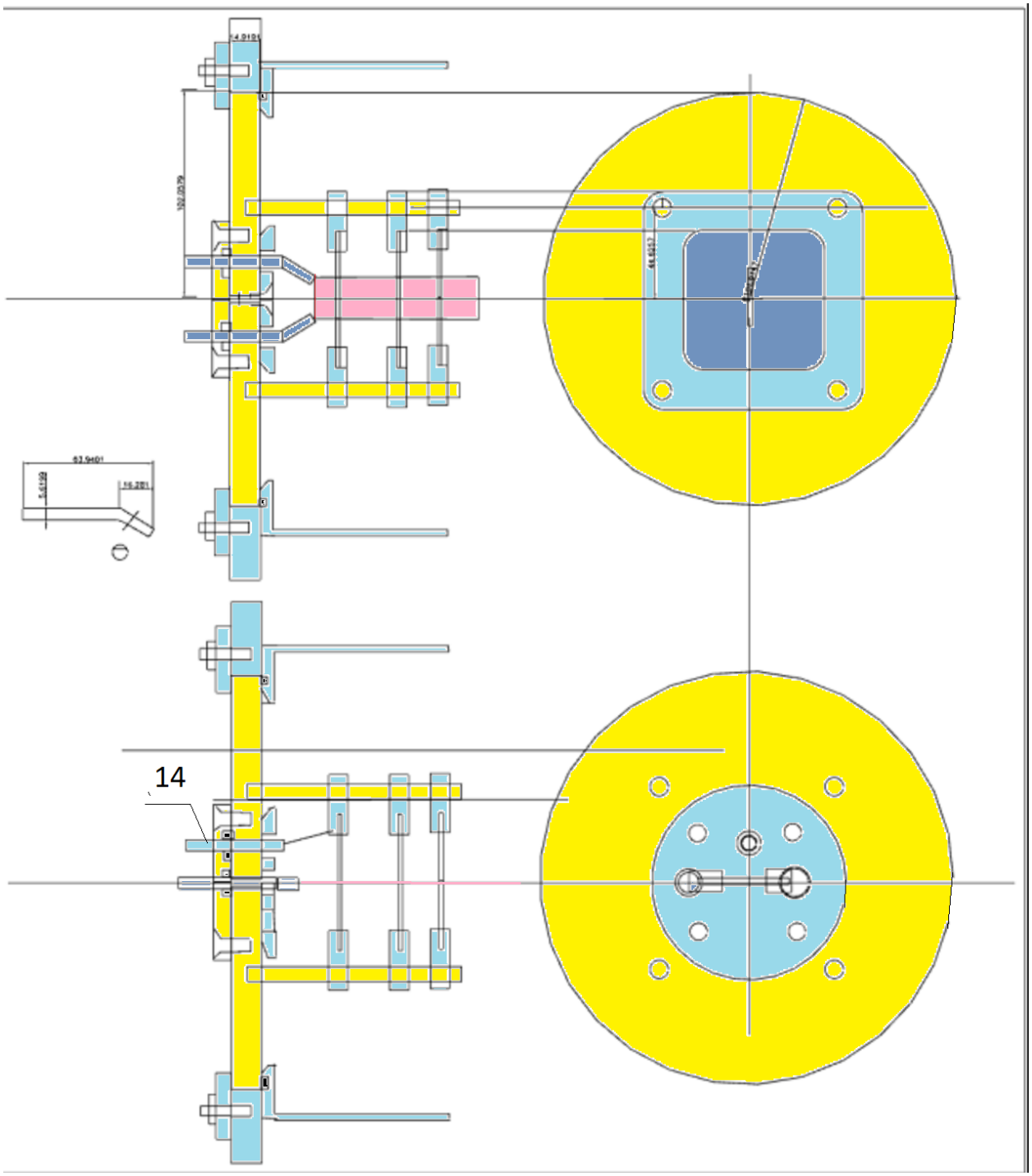

Fig. 11. Projections of electron gun

2) Specific Resistance of Ir ρ~60 μΩ cm at 1400 K. Specific resistance of Ce is 75 μΩ cm. Cross section of emitter S=0.1x2 mm^2=0.002 cm^2, length of emitter L~ 2 cm. Specific resistance of IrCe ~100 μΩ cm at 1400 K.

Resistance of emitter R= ρL/S=100 2/0.002=100 1000 μΩ=0.1 Ω.
P=R I^2. I^2=P/R=7/0.1=70 A^2. Heating current is I~8.4 A.

Two projections of electron gun are presented in Fig. 11.

Design of the IrCe emitter is presented in Fig. 12.

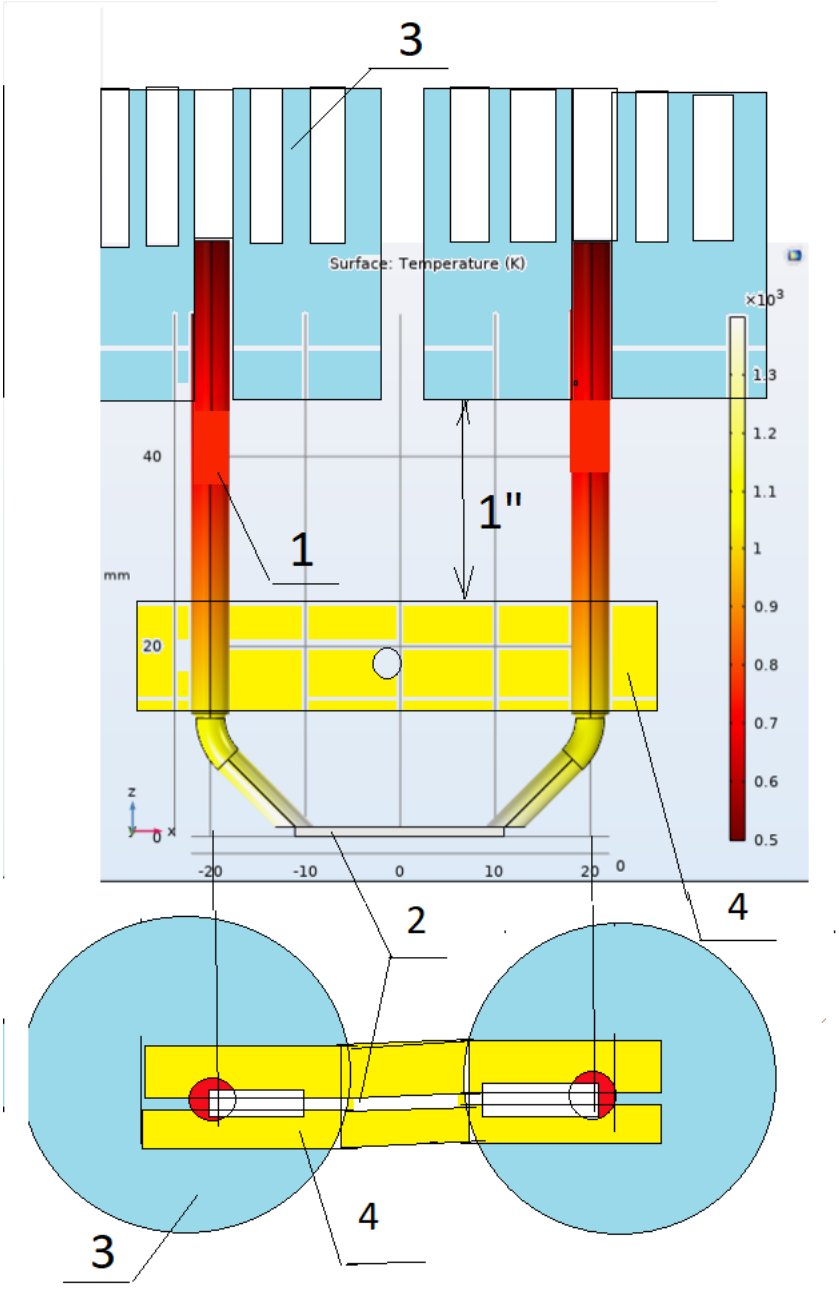

Fig. 12. Design of emitter IrCe.
1-current leads, 2-IrCe emitter, 3-radiator, 4-compessing ceramic.

Computer simulation of electron beam formation in strip cathode electron gun

Computer simulation of electron beam formation in electron gun is shown in Fig. 13.

With extraction voltage 3 kV and acceleration voltage 50 kV it is possible to form an electron beam with thickness ~ 0.1 mm.

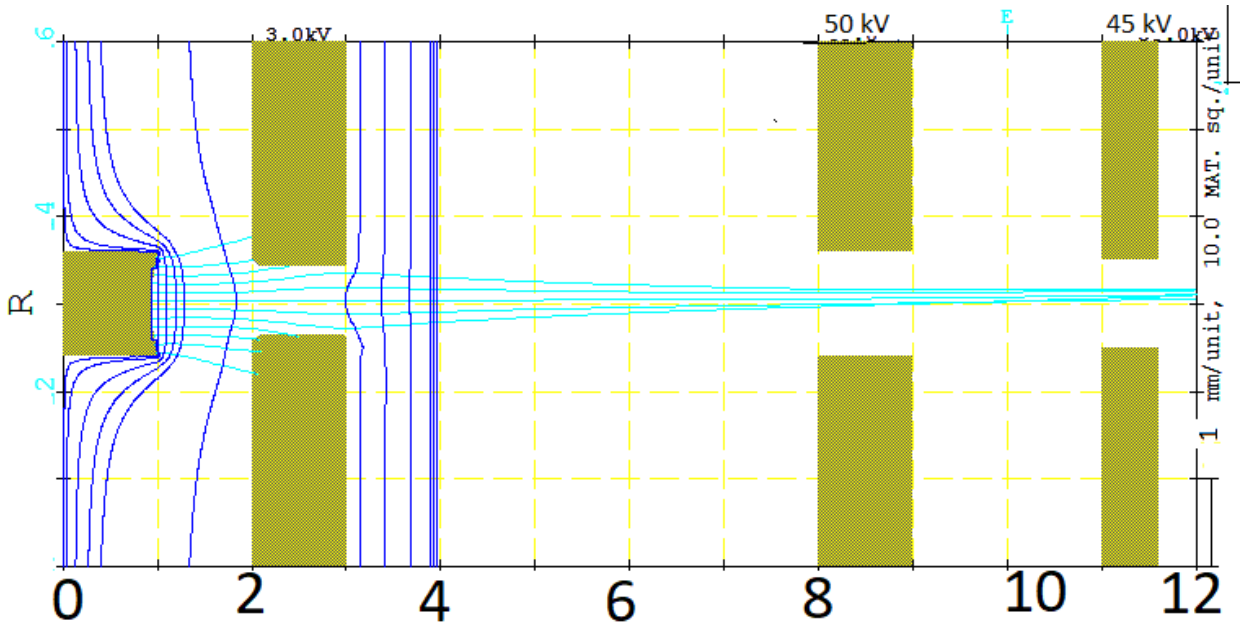

Fig. 13. Computer simulation of electron beam formation in electron gun.
Curvature radius of emitter is 5 mm.

Design of electron emitter consist of 1-current leads, 2-IrCe electron emitter with cross section 0.1x2 mm, 3-radiators, 4-compressing ceramic.

Emission current density of IrCe emitter can be up to 15 A/cm^2., from emitter of 2 mm width it can be 3A/cm=2 10^{19} electron/ cm sec=2 10^{10} electrons/cm nanosecond which can be visible in luminescent screen.

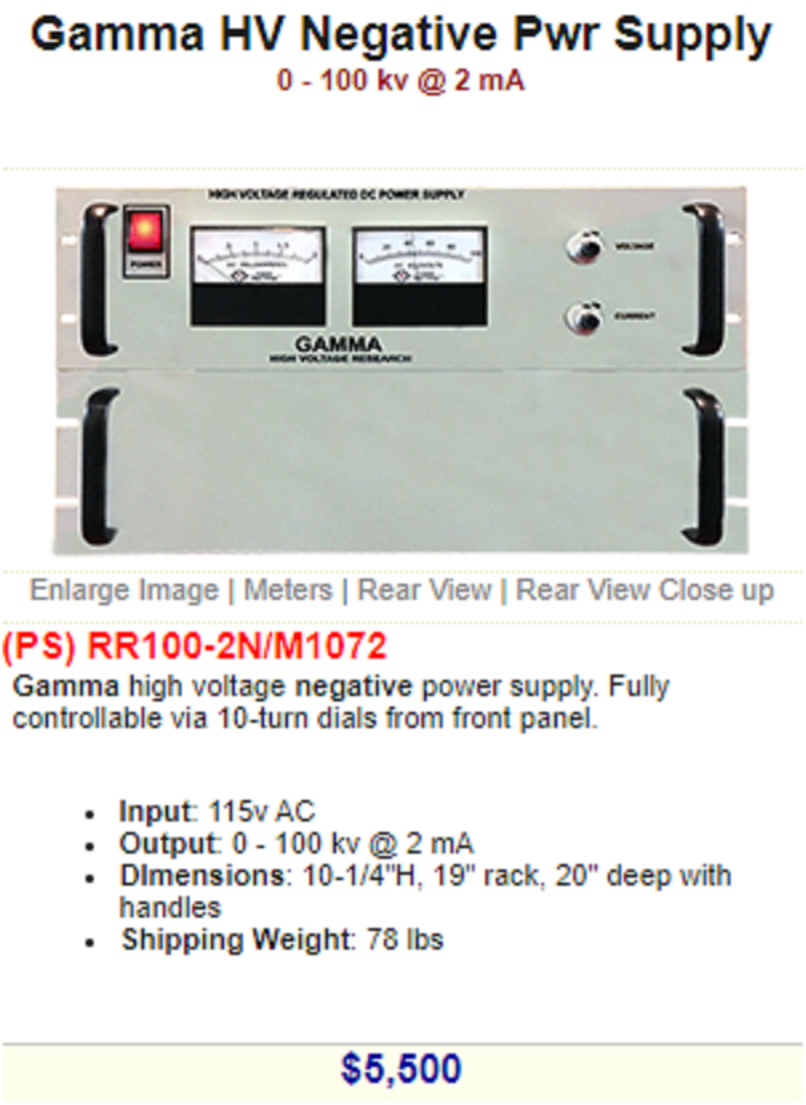

Fig. 14. High voltage power supply for electron beam acceleration

Power supply for sheet electron beam production

Fig. 15. Power supplies for sheet electron beam generation.

The high voltage power supplies for sheet electron beam generation are commercially available power supplies with voltage 100-160 kV and DC current up to 7.5 mA. The electron beam extraction uses a nanosecond generator with voltage up to 1 kV.

Luminescent screen

For increased sensitivity of the luminescent screen it is possible to use the luminescent screen with microchannel plates (MCP) as shown in Fig.16.

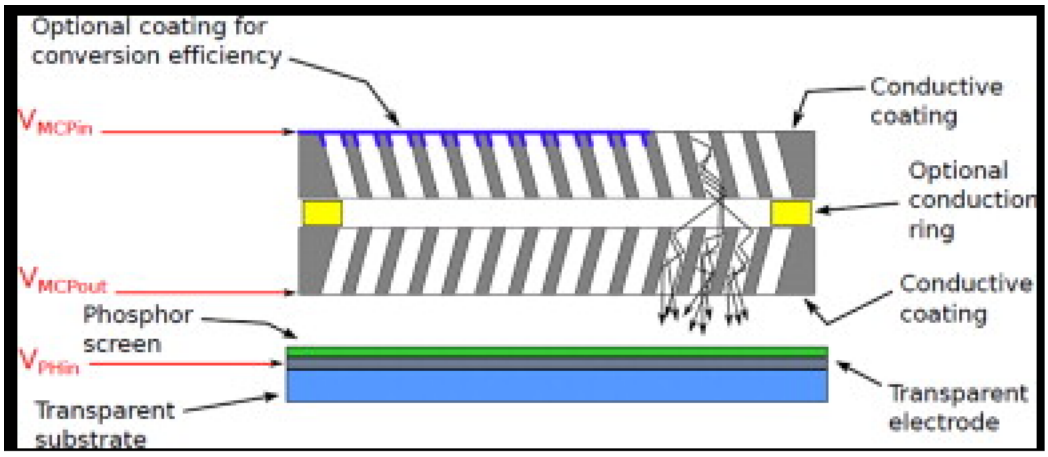

Fig.16. Luminescent screen with MCP.

The luminescent screen is augmented by two MCPs with conductive surfaces as shown on Fig. 16. Between conductive surfaces of MCP is applied pulsed voltage ~1 kV. Between the last MCP surface and conductive surfaces of the luminescent screen applied pulsed voltage ~ 6 kV for electrons acceleration into screen. One electron can be detected by this system [11]. MCP examples with dimensions 60x40 mm are shown in Fig.17.

Fig. 17. Examples of MCP with dimensions 60x40 mm.

An example of an assembled MCP is shown in Fig. 18.

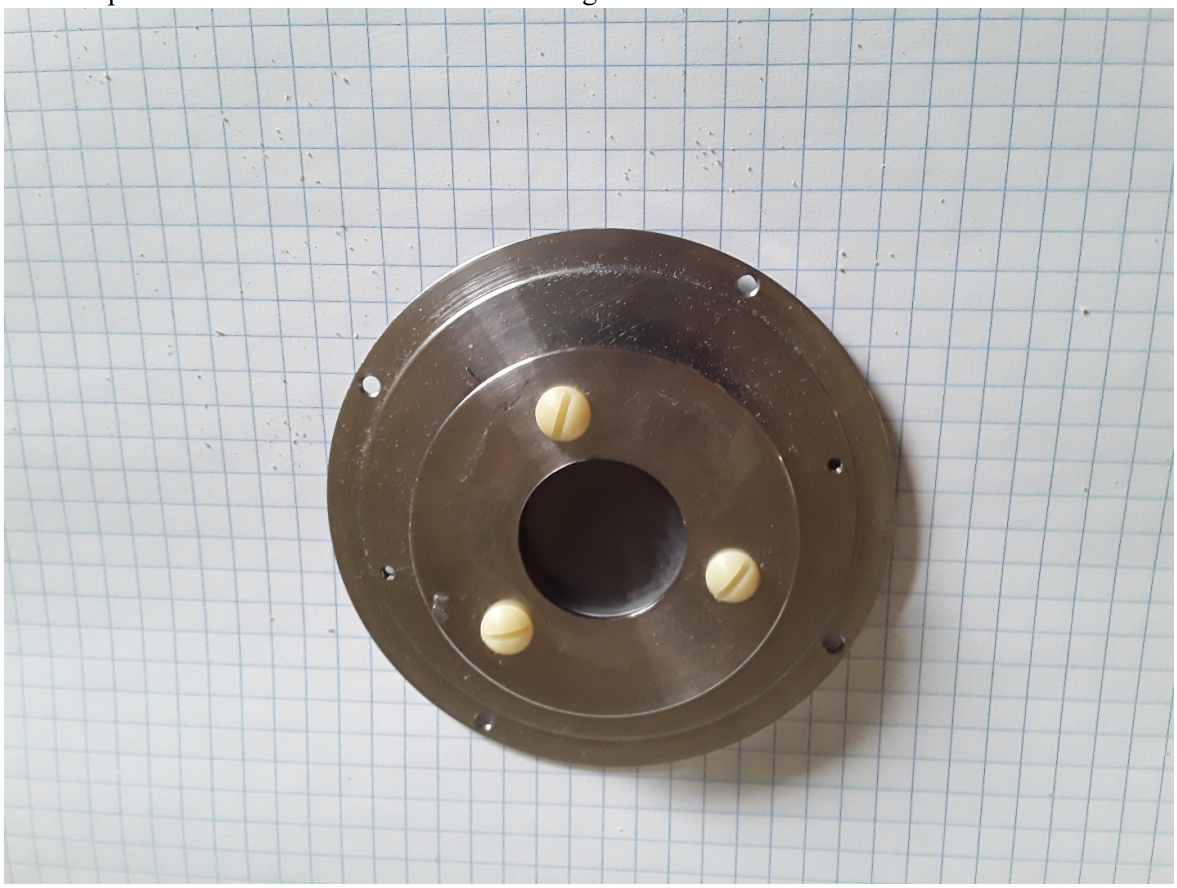

Fig. 18. Example of assembled MCP.

HAMAMATSU MCP luminescent screen assembly is shown in Fig. 18.
https://www.hamamatsu.com/resources/pdf/etd/MCP_assembly_TMCP0003E.pdf

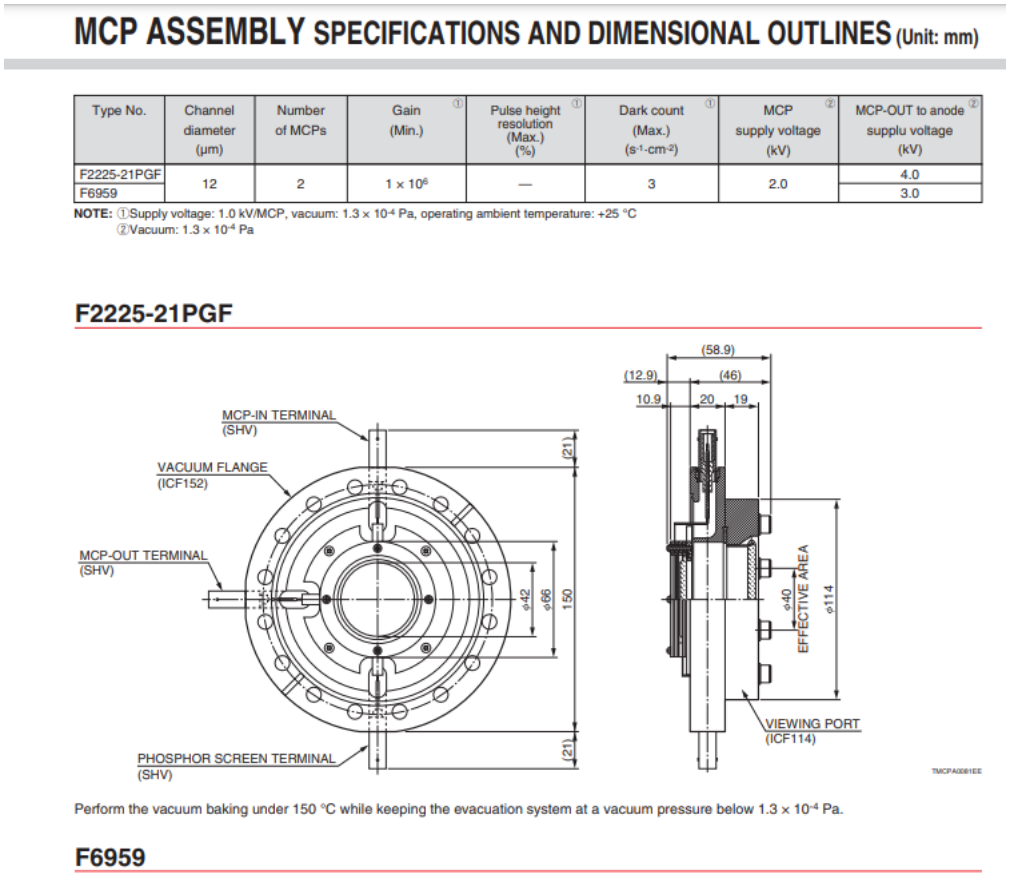

MCP ASSEMBLY SPECIFICATIONS AND DIMENSIONAL OUTLINES (Unit: mm)

Type No.	Channel diameter (μm)	Number of MCPs	Gain (Min.) ①	Pulse height resolution (Max.) (%) ①	Dark count (Max.) (s^{-1}-cm^{-2}) ①	MCP supply voltage (kV) ②	MCP-OUT to anode supplu voltage (kV) ②
F2225-21PGF	12	2	1×10^6	—	3	2.0	4.0
F6959							3.0

NOTE: ①Supply voltage: 1.0 kV/MCP, vacuum: 1.3×10^{-4} Pa, operating ambient temperature: +25 °C
②Vacuum: 1.3×10^{-4} Pa

F2225-21PGF

Perform the vacuum baking under 150 °C while keeping the evacuation system at a vacuum pressure below 1.3×10^{-4} Pa.

F6959

Fig. 19. HAMAMATSU MCP luminescent screen assembly.

Software for the SEPBPM operation and tomography image presentation will be improved for fast and reliable diagnostic operation.

Parameters of proton bunches in the Electron Ion Collider (EIC) are shown in Table 1. The bunch contains ~2 10^{11} protons with energy ~275 GeV, with RMS dimensions wxdxl =120x11 μmx6 cm. No. of bunches is 290, average current ~1 A. For estimation of the potential difference between the center of a bunches and the edge, it is possible to use a model with a uniform charge distribution. For a flat bunch electric field $E=4\pi\rho z$ and potential $\phi=4\pi\rho z^2/2=2\pi qd$. The proton density $n=210^{11}/0.12x0.011x60$ mm=2.5 10^{14} p/cm^3. The charge density $\rho=en=1.2\ 10^5$ cgse/cm^3, $\phi=4\pi\rho z^2/2=2\pi qd$ = 600 V. The transverse electric field of relativistic particles is γ times higher than that of a rest particle and the longitudinal field is γ^2 times weaker than in particle rest frame, where $\gamma=[1-(v/c)^2]^{-1/2}$.

The potential of a relativistic bunch with γ =150 is $\phi1=\gamma\ \phi=150\ 600=90$ kV.

An electron beam with energy W~100 keV is necessary for diagnostics of such bunches.

Table 1.: EIC beam parameters for different center-of-mass energies Vs, with strong hadron cooling. High divergence configuration

Species Energy [GeV]	proton 275
Bunch intensity [10^{10}]	19.1
No. of bunches	290
Beam current [A]	0.69
Emit., rms h/v [μm]	5.2/0.47
RMS emittance, h/v [nm]	18/1.6
beam size, h/v [μm]	119/11
RMS bunch length [cm]	6
Max. space charge	0.007

The electric field of a 3D Gaussian distribution is presented in Ref. [14] which gives for the potential:

$$\varphi_b = Q\,(2/\pi)^{1/2}/4\pi\varepsilon o\, r\,(\sigma_x\,\sigma_y\,\sigma_{z,b})\,\{\int_o^\infty d\lambda\,(e^{-x\,2\lambda^2/\,2(\lambda 2\sigma 2\,x+1)})\,(e^{-y\,2\lambda^2/\,2(\lambda 2\sigma 2\,y+1)})$$

$$(e^{-z\,2\lambda^2/\,2(\lambda 2\sigma 2\,z,b+1)})\,/\,[(\lambda^2+\sigma^{-2}x)^{1/2}\,(\lambda^2+\sigma^{-2}y)^{1/2}\,(\lambda^2+\sigma^{-2}zb)^{1/2}]\}$$

A possible solution comes from ATI with a full line of flash X-ray systems. These include systems with a nominal voltage of 150 kV, 300 kV, 450 kV, the largest commercially available.

Computer simulation development

Sheet profile meter for intense ion bunch.

Application of a sheet electron beam for scanning the cross-section of an intense ion beam is proposed. The transverse electric field of a ion bunch deflected the electrons of the testing beam. By measuring the deflection of the testing beam as a function of the displacement of its axis, one can get an idea of the profile of the ion beam. In the frame of project

1. computer code for simulation of sheet electron beam deflection by ultra-relativistic proton bunches was developed,
2. the simulation of deflection of sheet electron beam by ultra-relativistic proton bunches was performed.

Code SCAPRO

Introduction.

Currently experiments in the field of high-energy physics for fundamental and applied research require a constant increase in the intensity and brightness of charged particle beams and developing new methods for their diagnosis [1]. Such an improvement can be achieved on the basis of methods for diagnosing charged particle beams that do not worsen the quality of the studied beam. A significant role is played by non-invasive diagnostic methods that can be continuously used with intense beams of accelerated particles. One of the possibilities for diagnosing and measuring the parameters of intense bunch of charged particles is based on the use of a low-energy electron beam-a beam sensor [2-3]. A beam sensor is a device based on the use of a low-energy electron beam as

a tool for studying intense bunches of charged particles. The possibility of measuring the parameters of intense bunches by an electron beam is due to the deflection of the electrons of the testing beam by a certain angle in the fields of the studied bunches. The values of these deflection angles determine the distribution of the testing charged particles on the observed plane and the projection of the electron beam on the luminescent screen is sensitive to the shape of the proton bunch. The possibilities of this method of non-destructive diagnostics can be fully used only with a detailed study of the process of electron beam-proton bunch interaction. Since the problem of the motion of a beam of charged particles in electromagnetic fields cannot be solved analytically in general, for studying the structure of the beam, numerical modeling is a method that plays an essential role in experiments. The numerical simulations are also of significant importance in the interpretation of images obtained on the device screen. The results of experiment and computer simulation to determine the density distributions of accelerated particles by a scanning electron pencil beam are presented in paper [4]. However, the electron pencil beam device used is large and complex and makes it difficult to use this technique for accelerated beam diagnostics. This paper presents a numerical model and a results of computer simulation of the interaction of the testing sheet electron beam and the relativistic proton bunch. Instead of a scanning pencil electron beam we use a sheet electron beam that can be created by a strip cathode. The apparatus with the strip cathode has better accuracy of measurement and better time resolution [5]. As a results of simulation the dependence of the electron beam deflection on its energy, the angle of inclination to the direction of the proton bunch, the magnitude of the space charge and the velocity of the proton bunch is investigated.

The SCAPRO program is designed to simulate the deflection of a sheet electron beam by ultrarelativistic proton bunch. It is written in FORTRAN 77 and can be run on any PC with OC WINDOWS. The equations to be solved are written in Cartesian coordinates. The calculated area has the form of a parallelepiped. The maximum size of the region, the number of emitted electron beamlets of the cathode, and the accuracy of the solution are determined by the speed and memory of the PC. There are no additional restrictions on the size of the area in the program. For the parameters shown in Table 2, the SCAPRO program runs for only 5 minutes on a PC with an Intel(R) Core (TM) i7-6500U processor with a frequency of 2.59 GHz. No graphics package includes. The simulation results are output to files with formatted data, which allows you to draw a graph using Microsoft Excel or another visualization program To visualize the presented simulation results, the program TECPLOT 360 2010 was used (https://www.tecplot.com).

I. Statement of the sheet beam problem scanning profile meter for intense ion bunch.

We need to find an electron beam deflection by ultra-relativistic proton bunch. The diagram for measuring the beam profile as well as simulation domain for the 3-dimensional model are shown in the Fig. 1. Cartesian coordinates and the CGSE system of units are used. The size of a computational domain is $X_{max}=2k$, $Y_{max}=2l$, $Z_{max}=d+h$. At the beginning of the simulation a sheet electron beam emitted by cathode of width L and zero thickness. The electron beam intersects the proton bunch at an angle $\theta = 90^0-\alpha$ to the beam axis. Emitted by cathode a sheet electron beam is treated as a set of Np non-relativistic electron beamlets (macroparticles). The motion of each macroparticle is tracked by calculating the equation of motion.

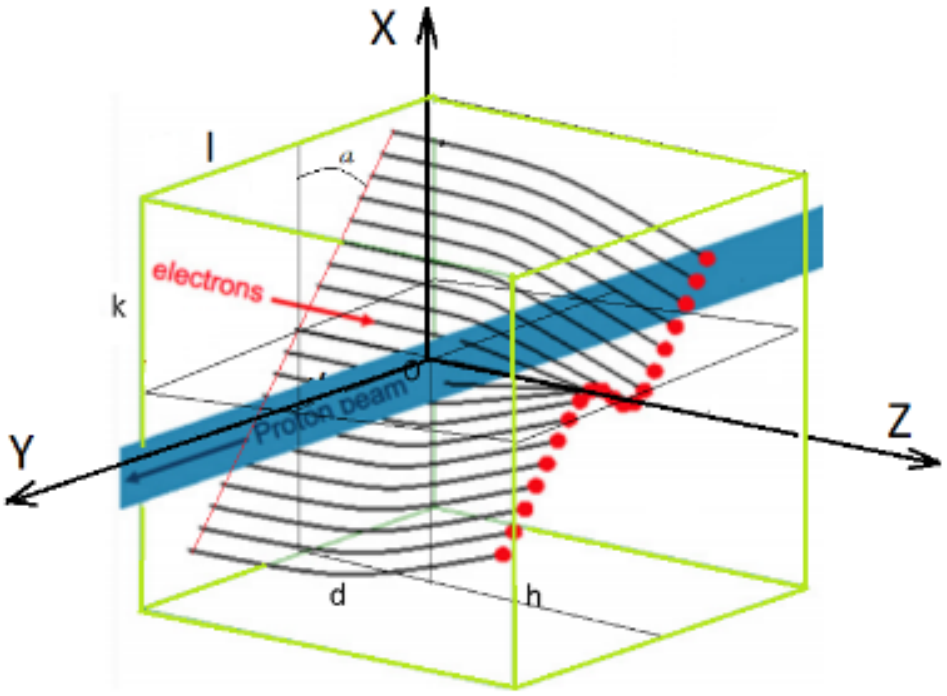

Fig. 1. Isometric view of a proton beam profile monitor with a ribbon probe.

The cathode is located in x-y plane at a distance z= - d from the center of the relativistic proton bunch. Electrons are launched from the cathode line with the velocity parallel to the z axis: $\boldsymbol{v}$= (v_x, v_y, v_z),

$$v_z = \sqrt{2W/m}\,, \quad v_x=0, \quad v_y = 0, \qquad (1)$$

where c=3 10^{10} cm/s is speed of light, m = 0.91 * 10^{-27} g is the electron mass, W is the electron beam energy in erg (1eV = 1.6 10^{-12} erg). The electrons are deflected by the electric field of the space charge and by the magnetic field of the relativistic proton bunch and are received by a luminescent screen in the x-y plane at a distance z= h from the center of the proton bunch. The model used to solve the problem consists of the equations of motion of the electron beam under the action of an electromagnetic field created by a relativistic proton bunch. The beam is modeled by calculating of electron trajectories (Np) passing through the computational domain. Each trajectory is computed independent of all the others. To find the potential, the Poisson equation is solved.

The test runs were carried out for the size computational domain k=2 cm, l=2 cm, d=2 cm, h=4 cm, the electron beam size L=1 cm, the angle between cathode and x-axis α= 45^0, the electron beam energy W=30÷200 keV. Parameters assumed for the simulation are presented in Table 2.

II. Set up of mathematical model.

1. The equations of motion of electrons:

$$m\frac{d\boldsymbol{v}}{dt} = e\boldsymbol{E} + \frac{e}{c}[\boldsymbol{vB}] \qquad (2)$$

$$m\frac{dv_x}{dt} = e\gamma E_x + \frac{e}{c}(v_y B_z - v_z B_x) \quad (3)$$

$$m\frac{dv_y}{dt} = eE_y + \frac{e}{c}(v_z B_x - v_x B_z) \quad (4)$$

$$m\frac{dv_z}{dt} = e\gamma E_z + \frac{e}{c}(v_x B_y - v_y B_x) \quad (5)$$

$$\frac{d\boldsymbol{X}}{dt} = \boldsymbol{v}, \qquad \boldsymbol{X} = (x, y, z), \qquad \boldsymbol{v} = (v_x, v_y, v_z) \quad (6)$$

$$B_x = \beta\gamma E_y, \; B_y = 0, \; B_z = \beta\gamma E_x, \; \gamma = \frac{1}{\sqrt{1-\beta^2}} \quad (7)$$

Here v_x , v_y , v_z are the components of the electron velocity in cm / s, e= - 4.8 10^{-10} is the electron charge in CGSE units, c=3 10^{10} cm/s is a speed of light, E_x , E_y , E_z and B_x , B_y , B_z are the components of the electric field and magnetic field created by a space charge of the proton bunch, $\gamma = \frac{1}{\sqrt{1-\beta^2}}$ is a relativistic factor of the proton beam , β= u/c = $(1\text{-}1/\gamma^2)^{1/2}$ is the dimensionless velocity of the proton bunch. Electric field and magnetic field are expressed in CGSE units. Taking into account the condition v_x , v_y << v_z , the equations of motion of electrons have the form:

$$m\frac{dv_x}{dt} = -e\gamma E_x \quad (8)$$

$$m\frac{dv_y}{dt} = -eE_y\left(1 + \gamma\frac{v_z\beta}{c}\right) \quad (9)$$

$$m\frac{dv_z}{dt} = -e\gamma E_z \quad (10)$$

$$\frac{dx}{dt} = v_x, \qquad \frac{dy}{dt} = v_y, \qquad \frac{dz}{dt} = v_z \quad (11)$$

2. The charge density of the relativistic proton bunch is determined by the formula:

$$\rho(x, y, z) = \frac{Q}{84abc\pi^{\frac{3}{2}}} \exp\left[-\left(\frac{x^2}{a^2} + \frac{y^2}{b^2} + \frac{z^2}{C^2}\right)\right] \quad (12)$$

Here Q is the charge of proton bunch and a, b, C are the sizes of the bunch. Proton bunch parameters are: 1<γ< 250, 0.01mm < a<2.0 mm, b=60 mm, 0.01mm < C < 2.0 mm, Q=$4.8\cdot10^{-10}$ N (CGSE), N=$2\cdot10^{10}\div2\cdot10^{11}$.

3. The electric field is found from the solution of the Poisson equation**:**

$$\frac{\partial^2\varphi}{\partial x^2} + \frac{\partial^2\varphi}{\partial y^2} + \frac{\partial^2\varphi}{\partial z^2} = -4\pi\rho(x, y, z) \quad (13)$$

$$E_x = -\frac{\partial\varphi}{\partial x} \quad E_y = -\frac{\partial\varphi}{\partial y} \quad E_z = -\frac{\partial\varphi}{\partial z} \quad (14)$$

The planes x = + - k, y=+- l, z= - d, and z=h are conductive, so the boundary condition φ=0 is assumed. The electric field ***E*** and the magnetic field ***B*** are determined in accordance with the Lorentz transformation [6].

4. The dimensionless form of all equations.

To solve the problem, we use the dimensionless form of all equations. Let us use dimensionless variables: $v_x' = v_x/c$, $v_y' = v_y/c$, $v_z' = v_z/c$, $t' = t/t_0$, $E_x' = E_x/E_0$, $E_y' =$

$E_y/E_0,\ E_z' = E_z/E_0,\ \varphi' = \varphi/\varphi_0,\ \rho' = \rho/\rho_0,\ x' = x/L_0,\ y' = y/L_0,\ z' = z/L_0$. The values of the scales $c,\ t_0, E_0, \varphi_0, \rho_0, L_0$ are listed in Table 1.

Table 1.

Velocity	c=3 10^{10} cm/s - speed of light
Spatial size	L_0 =1 cm
Time	$t_0 = L_0/c$ =0.33 10^{-10} s
Electric field	$E_0 = \frac{mc}{et_0}$ =1.7 10^3 statvolt/cm = 5.1 10^5 v/cm
Potential	$\varphi_0 = \frac{mc^2}{e} =$ 1.7 10^3 statvolt =5.1 10^5 v
Charge density	$\rho_0 = \frac{m}{4\pi e t_0^2}$ =1.36 10^2 statcoulomb/cm^3 = 0.045 Coulomb/m^3

The dimensionless form of equations (8) – (10), (13) are:

$$\frac{dv_x'}{dt'} = -\gamma E_x' \qquad (8')$$

$$\frac{dv_y'}{dt'} = -E_y'(1 + \gamma\beta v_z') \qquad (9')$$

$$\frac{dv_z'}{dt'} = -\gamma E_z' \qquad (10')$$

$$\frac{\partial^2\varphi'}{\partial x'^2} + \frac{\partial^2\varphi'}{\partial y'^2} + \frac{\partial^2\varphi'}{\partial z'^2} = -\rho' \qquad (13')$$

The dimensionless form of equation (12) is:

$$\rho' = \frac{Q'}{a'b'c'}\exp\left[-\left(\frac{x'^2}{a'^2} + \frac{y'^2}{b'^2} + \frac{z'^2}{c'^2}\right)\right] \qquad (12'),$$

$$a' = \frac{a}{L_0},\ b' = \frac{b}{L_0},\quad c' = \frac{C}{L_0}.\quad Q' = \frac{Q}{84L_0^3\pi^{\frac{3}{2}}\rho_0} = \frac{e^2N}{21\sqrt{\pi}mc_0^2L_0}$$

Next, all formulas are given in dimensionless variables.

5. Algorithms of calculation.

a) Algorithm of calculating charge density of proton bunch on the regular grid with nodes $(x_i, y_{k,}\, z_l)$ is:

$$x_i = -x_m + (i-1)h_x,\quad i = 1, \dots, i_m,\quad h_x = \frac{2x_m}{i_m - 1}$$

$$y_k = -y_m + (k-1)h_y,\quad k = 1, \dots, k_m,\quad h_y = \frac{2y_m}{k_m - 1}$$

$$z_l = -z_m^1 + (l-1)h_z,\quad l = 1, \dots, l_m,\quad h_z = \frac{z_m^1 + z_m^2}{l_m - 1}$$

$$\overline{\rho}_{i,k,l} = \rho(x_i, y_k, z_l) = \frac{Q'}{abC}\exp\left[-\left(\frac{x_i^2}{a^2} + \frac{y_k^2}{b^2} + \frac{z_l^2}{C^2}\right)\right].$$

Calculating the potential are based on formula:

$$\frac{\varphi_{i+1} - 2\varphi + \varphi_{i-1}}{h_x^2} + \frac{\varphi_{k+1} - 2\varphi + \varphi_{k-1}}{h_y^2} + \frac{\varphi_{l+1} - 2\varphi + \varphi_{l-1}}{h_z^2} + \rho = 0$$

$$i = 2, \dots, i_m - 1,\quad k = 2, \dots, k_m - 1,\quad l = 2, \dots, l_m - 1$$

with boundary conditions:

$$\varphi_{boundary} = 0.$$

Upper relaxation method to calculate the potential φ was used.

$$\overline{\varphi} = \left[\frac{\varphi_{i+1}^n + \varphi_{i-1}^n}{h_x^2} + \frac{\varphi_{k+1}^n + \varphi_{k-1}^n}{h_y^2} + \frac{\varphi_{l+1}^n + \varphi_{l-1}^n}{h_z^2} + \rho\right]\left(\frac{2}{h_x^2} + \frac{2}{h_y^2} + \frac{2}{h_z^2}\right)^{-1}$$

$$\varphi^{n+1} = (1-\omega)\varphi^n + \omega\overline{\varphi}\ ,$$

n – iteration number, ω – iteration parameter ($\omega = 1.93$). Iterations are performed until the condition is met

$$\left|\varphi_{i,k,l}^{n+1} - \varphi_{i,k,l}^n\right| < \varepsilon, \quad \varepsilon = 10^{-10},$$

ε is a calculation accuracy.

b) Algorithm of the electric field calculation:

$$E_{x,i-\frac{1}{2}} = -\frac{\varphi - \varphi_{i-1}}{h_x}$$

$$E_{y,k-\frac{1}{2}} = -\frac{\varphi - \varphi_{k-1}}{h_y}$$

$$E_{z,l-\frac{1}{2}} = -\frac{\varphi - \varphi_{l-1}}{h_z}$$

c) Initial coordinates of the electron beam particles on the plane (x, y, z= - 2) are

$$x_n = A_x n + B_x, \quad y_n = A_y n + B_y, \quad z_n = -z_m^1.$$

$$A_x = \frac{x_2 - x_1}{N_p - 1}, \quad B_x = x_1 - A_x,$$

$$A_y = \frac{y_2 - y_1}{N_p - 1}, \quad B_y = y_1 - A_y,$$

where N_p is a number of trajectories, n is a trajectory number, $x_1 = -\frac{L}{2}\cos\alpha$, $y_1 = -\frac{L}{2}\sin\alpha$, $x_2 = \frac{L}{2}\cos\alpha$, $y_2 = \frac{L}{2}\sin\alpha$.

Initial velocities of electron beam at the initial time $t = 0$ are $(v_x, v_y, v_z) = (0, 0, \sqrt{2W/m})$.

d) Scheme for solving the particles motion equations.

Equations (8'), (9'), (10') have an analytical solution when the electric field **E**(x,y,z)=const:

$$v_x(t) = v_x^0 + \gamma E_x t$$

$$v_y(t) = v_y^0 + \gamma E_y(1 + \beta v_z^0)t + \frac{1}{2}\gamma^2\beta E_y E_z t^2$$

$$v_z(t) = v_z^0 + \gamma E_z t.$$

e) Algorithm to solve the particles motion equations includes 4 steps:

1. interpolation of the electric field components to the particle location: $\boldsymbol{E}(x^m,\ y^m,\ z^m) \equiv \{E_x, E_y, E_z\}$,
2. calculating the electron beam velocity

$$u_x^{m+1/2} = u_x^{m-1/2} + \gamma E_x$$

$$u_y^{m+1/2} = u_y^{m-1/2} + E_y\left(1 + \gamma\beta u_z^{m-1/2}\right)\tau + \frac{1}{2}\gamma^2\beta E_y E_z \tau^2$$

$$u_z^{m+1/2} = u_z^{m-1/2} + \gamma E_z \tau$$

3. calculating of new coordinates and time

$$x^{m+1} = x^m + \tau u_x^{m+1/2}$$

$$y^{m+1} = y^m + \tau u_y^{m+1/2}$$
$$z^{m+1} = z^m + \tau u_z^{m+1/2}$$
$$t^{m+1} = t^m + \tau,$$

where τ is the time step, m is the number of the time step.

4. end of calculations.

When the particle reaches the boundary of the calculation area ($z^{m+1} > z_m^2$) the coordinates and time of the intersection of the trajectory with the $z = z_m^2$ plane is calculated ($t = t_{end}$):

$$s = \frac{z_m^2 - z^m}{z^{m+1} - z^m}$$
$$x_{end} = x^m + s(x^{m+1} - x^m)$$
$$y_{end} = y^m + s(y^{m+1} - y^m)$$
$$t_{end} = t^m + \tau s.$$

We developed this method following the co-design approach [8,9].

III. Results of simulations beam deflection by proton bunch.

Parameters assumed for the simulation Run1 and Run2 are presented in Table 2.

Table 2.

	Run 1	Run2
Q, cul	$3.2\ 10^{-8}$	$3.2\ 10^{-8}$
N	$2\ 10^{11}$	$2\ 10^{11}$
a, cm	0.02	0.1
b, cm	6.0	6.0
C, cm	0.001	0.05
L, cm	2.0	2.0
θ, grad	45	45
W, keV	50	100
γ	100	100
Np	140	140
k=xm, cm	2.0	2.0
l= ym, cm	2.0	2.0
h=zm1, cm	2.0	2.0
d=zm2, cm	4.0	4.0
ntr	15	15
tau, $3.3\ 10^{-11}$ s	0.01	0.01
Grid [im, km, lm]	40x40x80	40x40x80

Here Q=eN is the charge of the proton bunch, N is the number of a proton in the bunch, a, b, C are the size of the bunch in cm, L is the size of the electron beam in cm, θ is the angle between cathode and proton bunch, W is the energy of electron beam in keV, gamma is γ- parameter of proton bunch. Parameters xm, ym zm1, and zm2 are the sizes of simulation box in cm (-xm < x < xm, -ym < y < ym, -zm1 < z < zm2). Number of the electron beamlets is Np, ntr is the number of output electron trajectories, tau is the time step, size of regular grid is [im, km, lm]. All startup parameters

can be entered in the std.sta file. To run the simulation, you need to use the executable program SCAPRO.exe.

The size of the regular grid [im, km, lm] and the number of electron beams Np can be changed in param.par file. You must use the Fortran compiler to get a new version of the executable program (SCAPRO.exe) with the new parameters Np, im, km, lm.
(http://simplyfortran.com/freetrial.html https://gcc.gnu.org/wiki/GFortran).

- **Results of computer simulation for Run1 presented at Fig. 2- Fig.9.**

The program TECPLOT 360 2010 was used for plotting the data (https://www.tecplot.com). 3D trajectories of deflected electron beamlets are shown in Fig. 2. A number of injected electron beamlets is Np=140, number of presented trajectories is ntr=30.

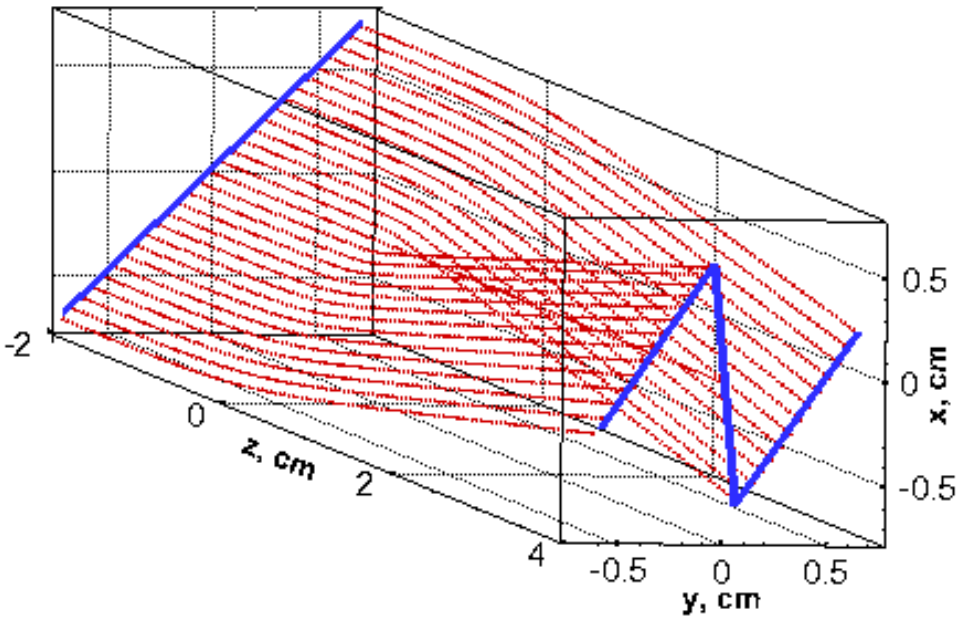

Fig.2. 3D trajectories of electron beam.

The projection of the electron beam trajectories on the (z-x) plane is shown in Fig. 3 ($0<t<t_{end}$).

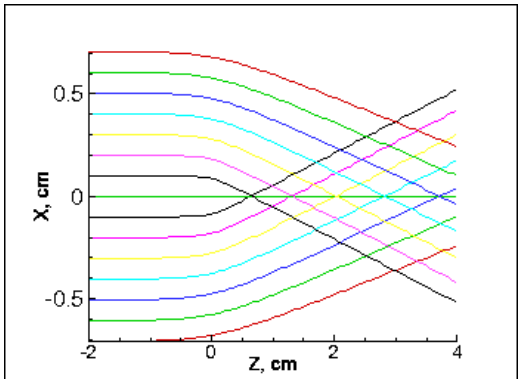

Fig.3. Projection of the trajectories of electron beam on plane (z-x) (0<t<t

Track of deflected electron beam on the luminescent screen z=4 is shown in Fig.4. Distance between max and min of curve Δy=0.078 cm is related to horizontal dimension of proton bunch. Amplitude of deflection Δx=1.11cm is proportional to number of protons and γ-factor of proton bunch and inverse proportional of electron beam energy.

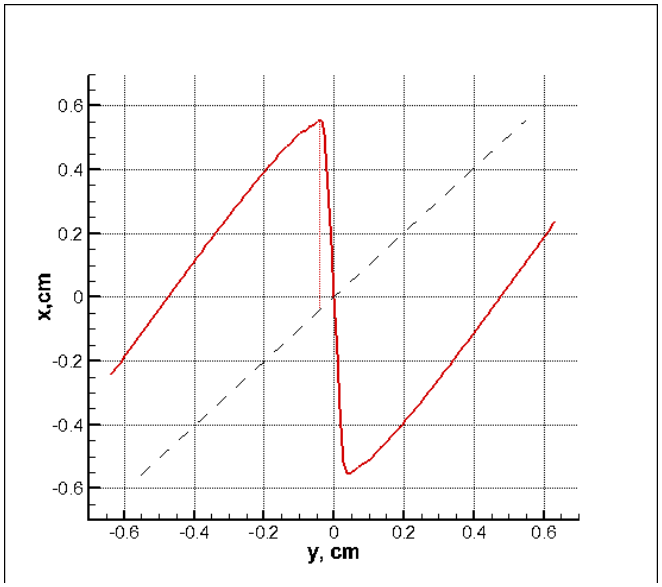

Fig.4. Track of deflected electron beam on the luminescent screen (z=4). Dashed line is trace of non-deflected electron beam.

The averaged spatial distributions of the electric field potential are shown in Fig.5 ($0<t<t_{end}$).

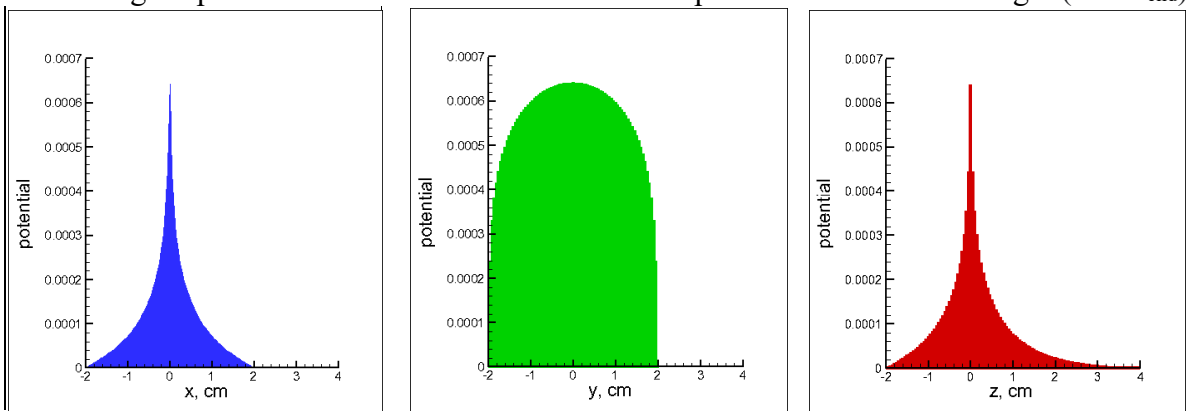

Fig.5. Averaged spatial distributions of the electric field potentials ($0<t<t_{end}$).

The dependence of the electron beam velocity components v_x, v_y, v_z on the z- coordinate ($0<t<t_{end}$) is shown in Fig. 6. The velosity is normalized to the speed of light $c=310^{10}$ cm/s.

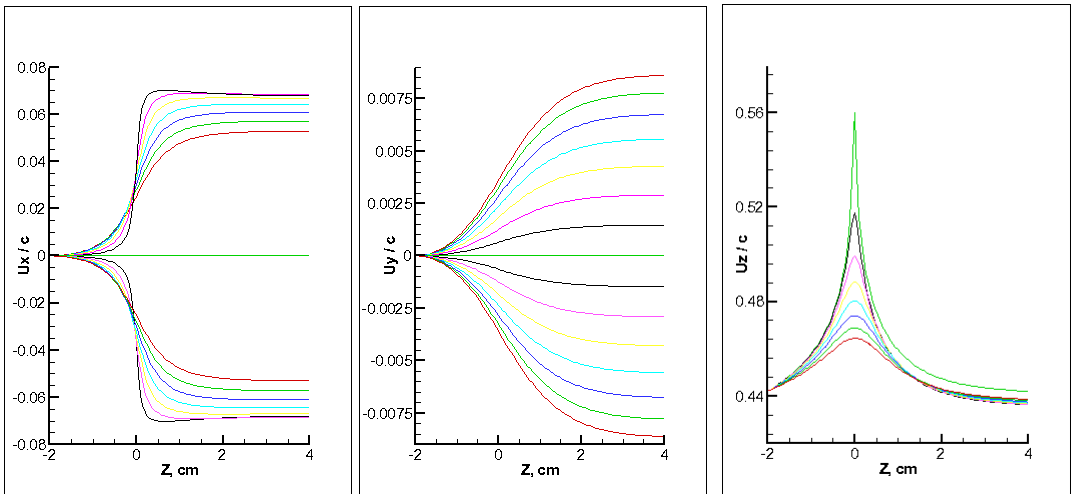

Fig. 6. Dependence of the electron beam velocity components on the z- coordinate ($0<t<t_{end}$).

The distribution of the proton bunch potential in the (y-z, x=0) plane is shown in Fig.7.

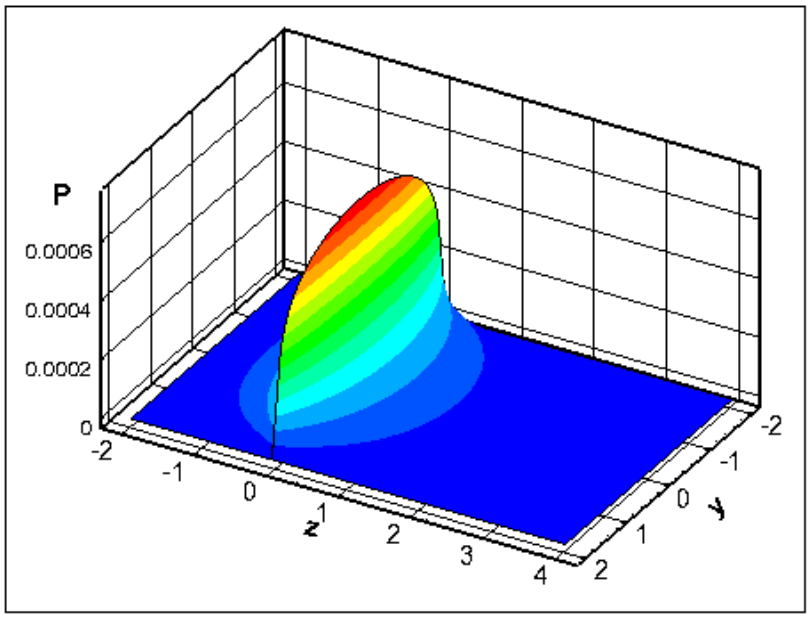

Fig. 7. 2D potential distribution of proton bunch at the plane x=0.

The spatial distribution of z-component of electric field Ez at the plane (y-z, x=0) is shown in Fig. 8. The spatial distribution of x-component of electric field Ex at the plane (y-z, x=0) is shown in Fig. 9.

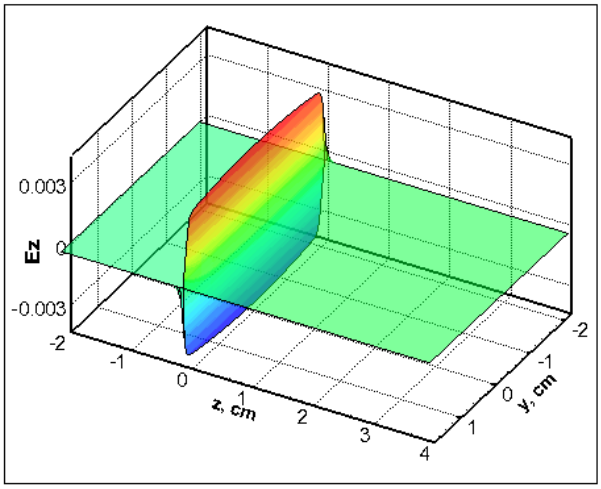

Fig. 8. Spatial distribution of z-component of electric field Ez at plane x=0.

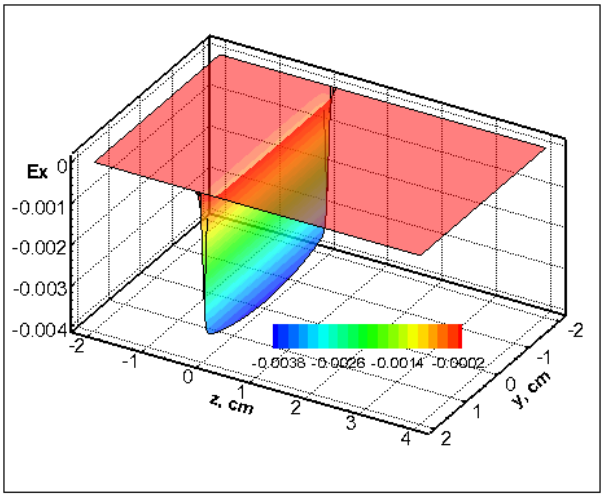

Fig. 9. Spatial distribution of x-component of electric field Ex at plane x=0.

- **Results of computer simulation for Run2 with increased transverse bunch size presented at Fig. 10- Fig. 19.**

3D trajectories of deflected electron beamlets are shown in Fig. 10. A number of injected electron beamlets is Np=140, number of presented trajectories is ntr=30.

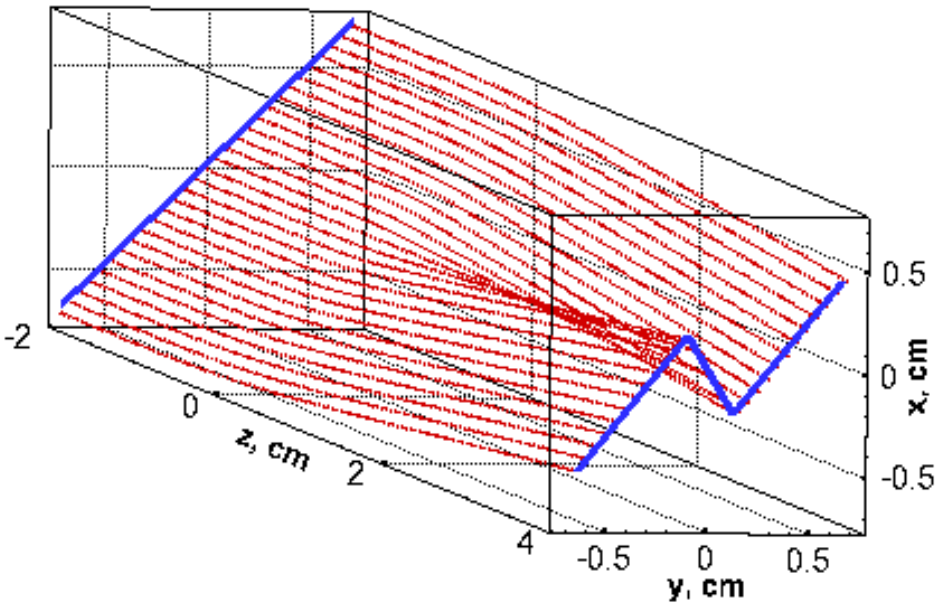

Fig.10. 3D trajectories of electron beam.

Projection of the trajectories of electron beamlets on a plane z-x is shown in Fig.11 ($0<t<t_{end}$).

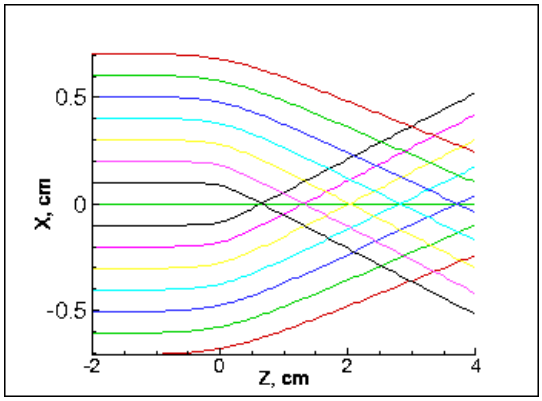

Fig.11. Projection of the trajectories of electron beam in plane z-x ($0<t<t_{end}$).

Track of deflected electron beam on the luminescent screen z=4 cm is shown in Fig.12. Dashed line is trace of non-deflected electron beam. Distance between max and min of blue curves $\Delta y=0.24$ cm is related to horizontal dimension of proton bunch. Amplitude of deflection $\Delta x=0.36$ cm is proportional to number of protons, γ-factor of proton bunch, and inverse proportional of electron beam energy.

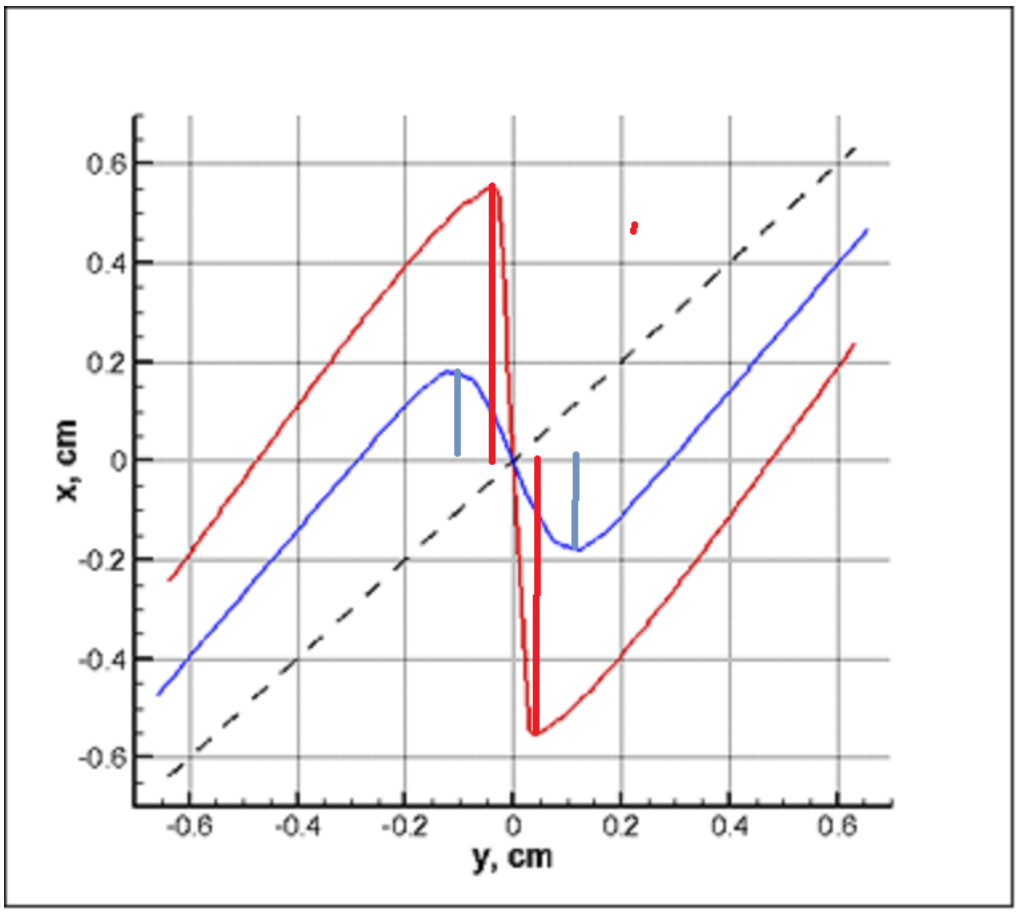

Fig.12. Tracks of deflected electron beam on the luminescent screen for RUN1-red, RUN2-blue. Dashed line is trace of non-deflected electron beam. Distance between max and min of blue curves $\Delta y=0.24$ cm is related to horizontal dimension of proton bunch. Amplitude of deflection $\Delta x=0.36$ cm is proportional to number of protons, γ-factor of proton bunch, and inverse proportional of electron beam energy.

The averaged spatial distributions of the potential are shown in Fig.13 ($0<t<t_{end}$).

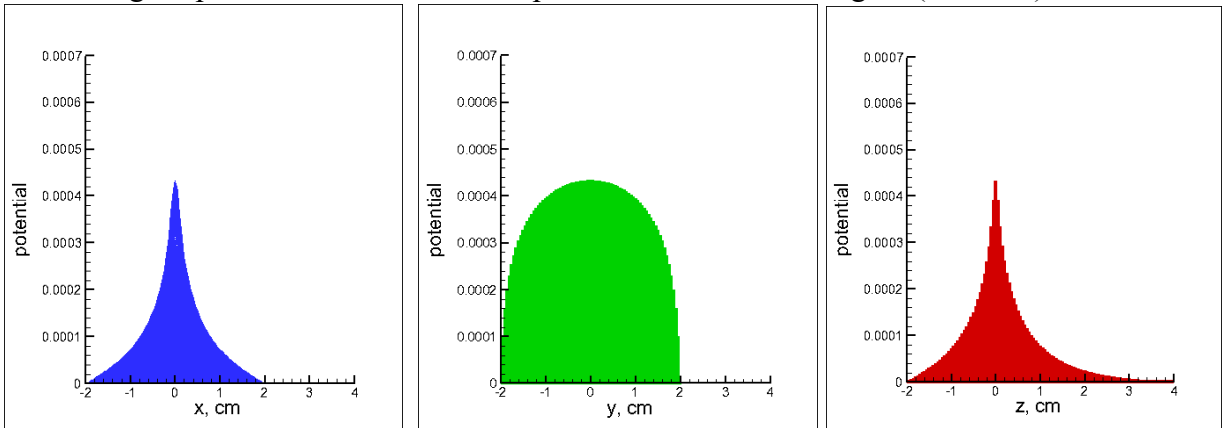

Fig.13. The averaged spatial distributions of the electric field potential ($0<t<t_{end}$).

The dependence of the electron beam velocity components v_x, v_y, v_z on the z- coordinate ($0<t<t_{end}$) is shown in Fig. 14. The velosity is normalized to the speed of light $c=310^{10}$ cm/s.

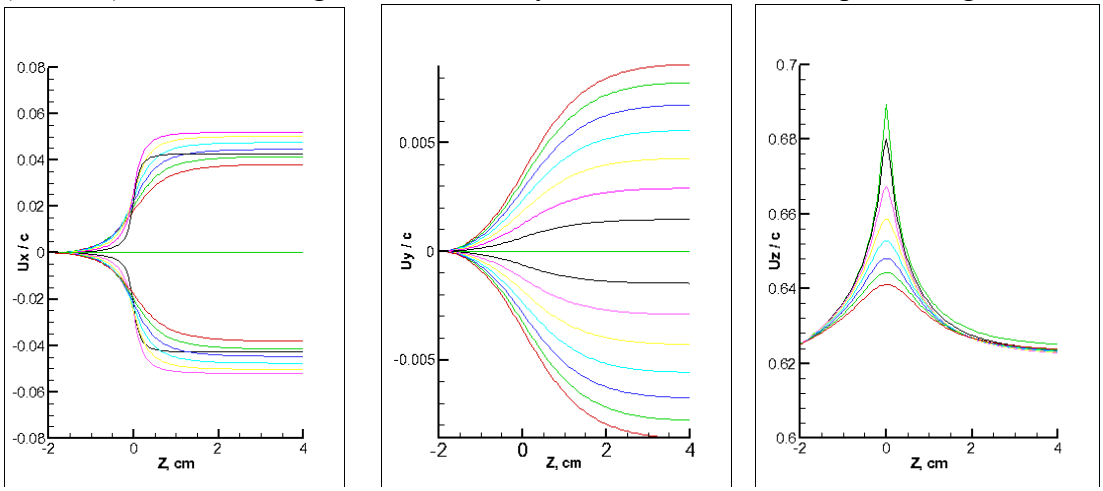

Fig. 14. Dependence of the electron beam velocity components on the z- coordinate ($0<t<t_{end}$).

The distribution of the proton beam potential in the (y-z, x=0) plane is shown in Fig.15.

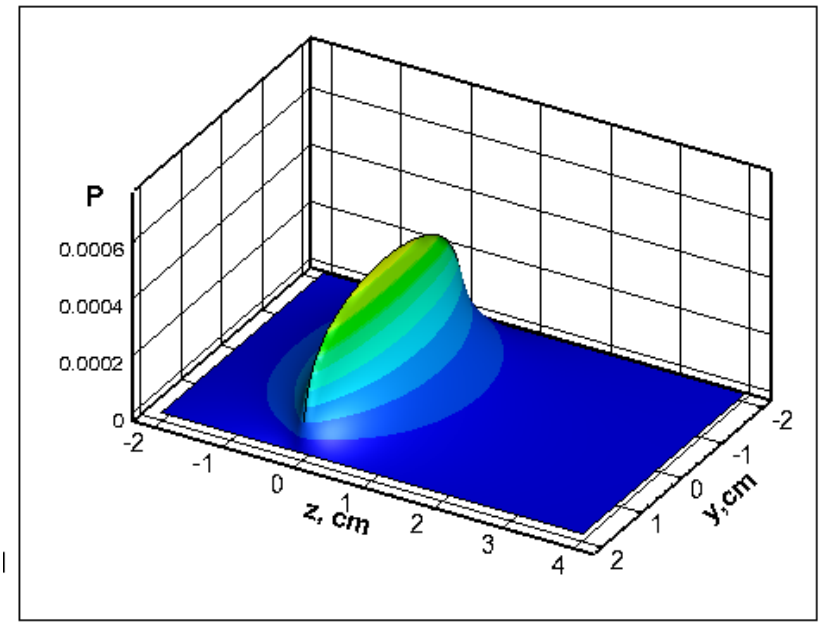

Fig. 15. Potential distribution of proton bunch at the plane x=0.

The spatial distribution of z-component of electric field Ez at plane (y-z, x=0) is shown in Fig. 16. The spatial distribution of x-component of electric field Ex at plane (y-z, x=0) is shown in Fig. 17.

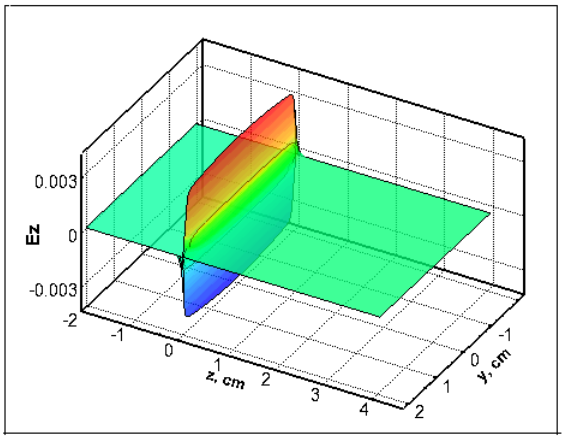

Fig. 16. Spatial distribution of z-component of electric field Ez at the plane x=0.

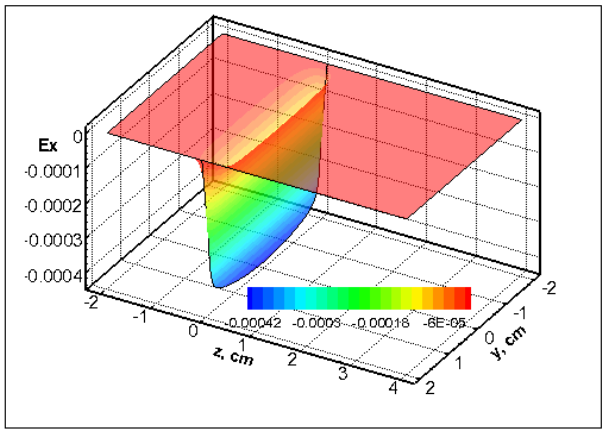

Fig. 17. Spatial distribution of x-component of electric field Ex at the plane x=0.

IV INTRODUCTION TO THE PROGRAM

Files used by the code SCAPRO include

- written in FORTRAN 77 SCAPRO.f file,
- executable program SCAPRO.exe file,
- the input data file std.sta (Fig.18),
- param.par file with the parameters of mesh (im, km, lm) and number of an electron beamlets Np (Fig. 19).

All parameters of run can be input in a file std. sta. Before start simulation open file std.sta and input parametes of simulation. Parameters a, b, C can be changed $0.01<a<0.3$, $6<b<10$, $0.005<C<0.3$, $10^9<an<10^{12}$, $30<W<200$, $1<gamma<200$, $0^0<\theta<90^0$, $1<ntr<140$, parameters xm=2, ym=2, zm1=2, zm2=4. Use file SCAPRO.exe to start the simulation. As a result of the program, the files fields.dat, std2.lst, ex.dat, ey.dat, ez.dat, potential.dat, std2.dat are created. The binary data file fields.dat contains information about the calculation in an unformatted form. File std2.lst presents parameters of simulation. The files ex.dat, ey.dat, ez.dat, potential.dat, std2.dat contain data with simulation results. Trajectory of electon beamlet with number K is presented in files trajectory00K.dat ($1<K<140$). All data are formatted and can be used to draw a plot. To visualize the calculation results, you can use Microsoft Excel or another visualization program. The example of plots obtained using Microsoft Excel is presented at Fig. 20. All calculations are done in double precision arithmetic. The accuracy of the program is derived directly by the resolution of the regular mesh. The size of space steps is hx=2xm/im, hy=2ym/km, hz=(2zm1+zm2)/lm (the parameters im, km, lm are located in the file param. par). You need to input size of time step τ into file std.sta according to conditions $\tau < \frac{\max(h_x,h_y,h_z)}{2v_z}$. To change the grid size (im, km, lm) or the number of beamlets (Np), you need to make changes to the param.par file (Fig. 19) and compile the program SCAPRO.f to get a new executable file SCAPRO.exe. The maximum size of the region, the number of emitted electron beams of the cathode, and the accuracy of the solution are determined by the speed and memory of the PC. There are no additional restrictions on the size of the area in the program.

For visualization of the calculation results, an additional executable program was created RIS.exe. It allows you to get the values of the potential and the components of the electric field in a given cross-section. The program TECPLOT 360 2010 was used to plot 2D graphs based on these data (Figs.7-9, Figs 15-17).

4. Results of computer simulation

Let us consider the results of computer simulations of the interaction of the testing sheet electron beam and the relativistic proton bunch.

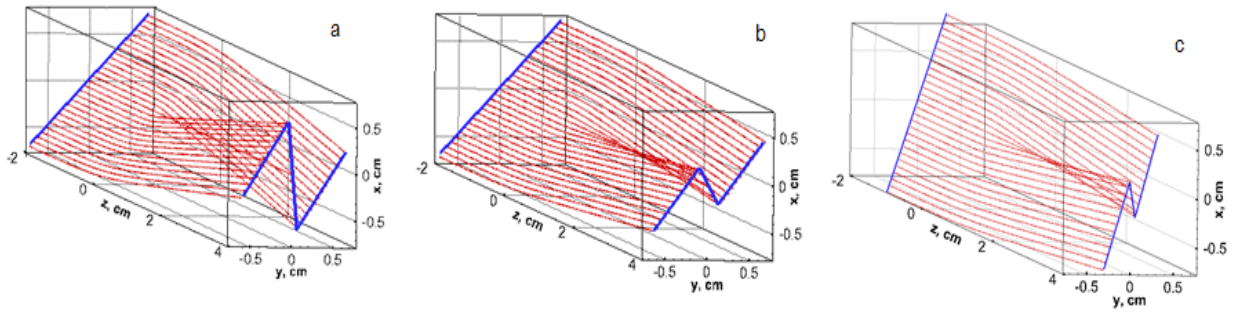

Fig.18. 3D trajectories of electron beam.

The trajectories of deflection electron probe beam by proton bunch with *γ=100* and number of proton $N=2\ 10^{11}$, $Q=3.2\ 10^{-8}$ *C* is shown In Fig. 2. The proton bunch has the dimensions: *a= 0.1 cm, b=6.0 cm, C =0.05 cm.* The parameters of electron beam are the next: *W=50 keV, θ=45º - (a); W=100 keV, θ=45º - (b); W=100 keV, θ=20º - (c).* The number of injected electron beamlets is *Np=140*, number of presented trajectories is *Ntr=30*. The projections of the electron beam on the cathode plane (*z=-2 cm*) and the plane of the luminescent screen (*z=4 cm*) are represented by blue

lines. These graphs show that with an increase in the energy of the electron beam *W*, there is a decrease in the amplitude of its deviation Δx by the relativistic proton bunch (Fig.18 a, b). From the comparison of Fig. 18 a and Fig. 18 c, it is seen that a decrease in the angle of inclination of the electron beam to the *x*-axis is accompanied by a decrease in the amplitude of its deviation Δx in the electromagnetic field created by a relativistic proton beam. Tracks of deflected electron beam on the luminescent screen *z=4* cm is shown in Fig.19. In the considered cases, the energy of the electron beams is equal to *100 keV*, the curves indicated by the numbers *1, 2, 3, 4, 5* correspond to the angle of inclination $\theta = 20^o, 30^o, 45^o, 60^o, 70^o$, accordingly. The dependence of the electron beam deflection size Δy (distances between maximum and minimum) on the angle of inclination θ is shown in Fig.20. In this way, with an increase in the angle of inclination of the cathode, the resolution of measuring the small transverse dimensions of the proton bunch can be significantly improved. The results of numerical modeling have shown that the amplitude of deflection Δx is proportional to the charge of proton bunch *Q* and the γ-factor of proton bunch. For example, when $Q = 1.6\ 10^{-8}$ C, $3.2\ 10^{-8}$ C, $4.8\ 10^{-8}$ C, the amplitudes of deflection Δx are *0.15 cm, 0.29 cm, 3.1 cm*, respectively. The dependence of the deviation Δx on the γ - factor of proton bunch is shown in Fig. 21 ($Q = 3.2\ 10^{-8}$ C). Thus, based on the obtained results of numerical modeling, it is possible to determine the parameters of the proton bunch by the displacement of the test electron beam on a screen.

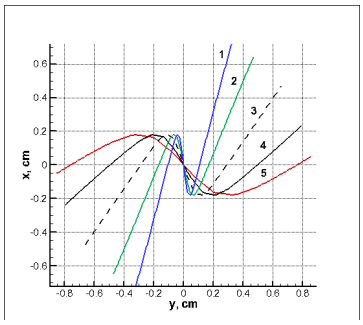

Fig.19. Tracks of deflected electron beam *a= 0.1 cm, b=6.0 cm, C =0.05 cm. θ =20º, 30º, 45º, 60º, 70º*

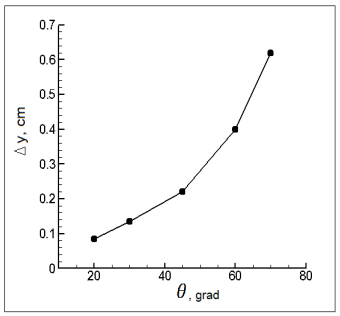

Fig.20. Dependence of beam deflection Δy on angle θ.

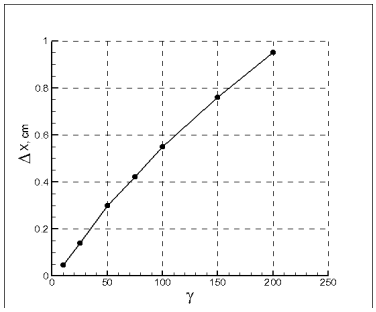

Fig.21. Dependence of deviation Δx on bunch γ-factor.

SCAPRO.exe file and the input data file std.sta are upload in site muonsinc.com weekly meeting.

*std2.sta - Notepad

File Edit Format View Help

```
2.d+11      an      !  Q=e*an
0.02d0      a       ! cm
6.d0        b       ! cm
1.d-3       C       ! cm
2.d0        dlk     ! size cathode (cm)
45.d0       alpha   ! angle cathode (grad)
50.d0       w       ! electron energy  (keV)
100.d0      gamma   ! gamma bunch
2.d0        xm      ! -xm < x < xm, cm
2.d0        ym      ! -ym < y < ym, cm
2.d0        zm1     ! -zm1 < z < zm2, cm
4.d0        zm2     ! cm
0.01d0      tau     ! time step
5           ntr     ! output tracks
1                   ! beamlet number 1
10                  ! beamlet number 10
75                  ! beamlet number 75
100                 ! beamlet number 100
130                 ! beamlet number 100
```

Fig.18. File std.sta.

param.par - Notepad

File Edit Format View Help

```
parameter(im=81,km=81,lm=121,Np=141)
```

Fig. 19. File param.par.

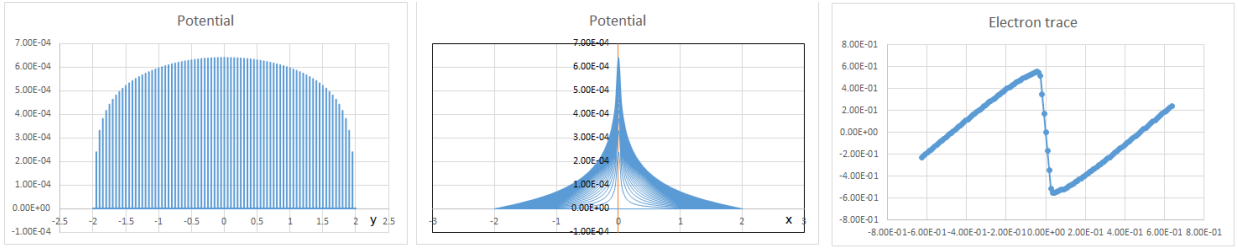

Fig. 20. Examples of visualizations obtained using Microsoft Excel.

Conclusion

A 3D numerical model of the interaction process of the testing electron beam and the proton bunch based on PIC method is created. The dependence of the electron beam deflection in the

electromagnetic field of a relativistic proton beam on the electron energy and the angle of inclination to the direction of the proton bunch is investigated. It is shown that the amplitude of the electron beam deflection is proportional to the charge and gamma factor of the proton bunch and inversely proportional to the energy of the electron beam. The obtained characteristics of the electron projection on the screen plane can be used to determine the main parameters of the relativistic proton bunch.

Test Stand Development

The sheet electron probe with electron beam extraction and beam characterization will be developed using a Test Stand that is an upgrade from the one used at ONRL to develop the H- ion source for the SNS.

Different views of the Test Stand are shown in Figs. 21-23.

Fig. 21. A test stand for electron beam testing (front left side) was designed, fabricated, assembled, and prepared for work. The Manual and Safety &Hazard instructions ware prepared, reviewed, and approved. The test stand was commissioned, and electron beam testing followed.

Fig. 22. Test stand for electron beam testing (front and right side). The high voltage parts are closed by metallic mesh shielding.

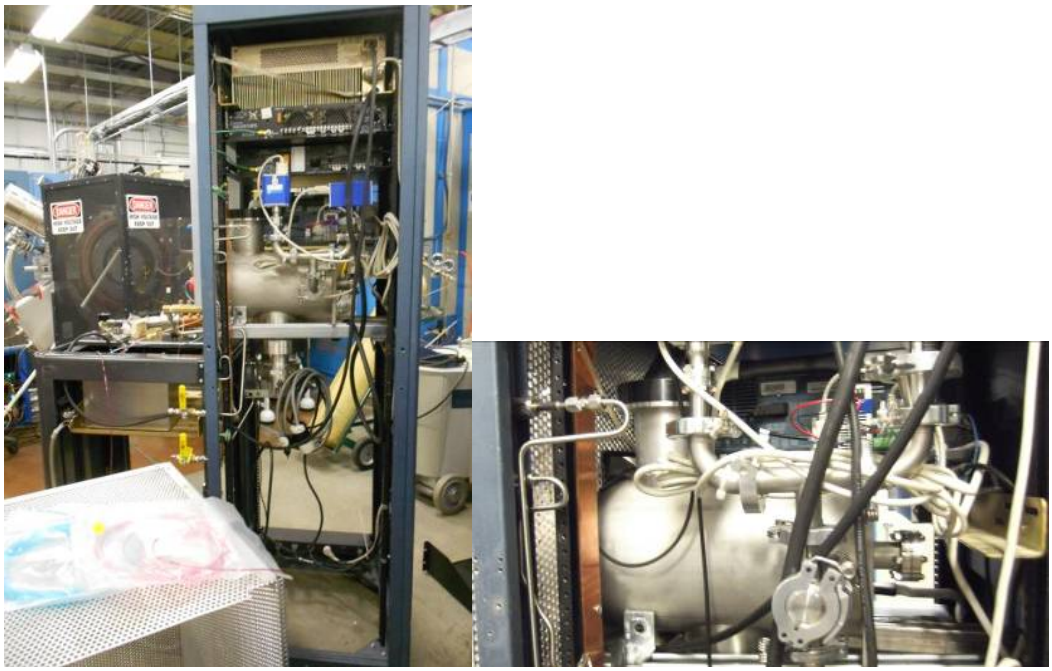

FIG. 23. Test stand for electron beam testing (rear side, shielding is removed). The electron source is attached to the vacuum chamber on the left side. Below is the vacuum chamber. The upper window can be used for beam formation observation. Below is a turbo molecular pump.

Anticipated Public Benefits

The proposed electron probe tomography system with the strip cathode should be the most advanced system for detailed diagnostics of accelerated beams. It can be used in all advanced accelerators and storage rings such as EIC, SNS, Main injector FNAL, RHIC, LHC, ISIS, KEK and many others. Serial production of these diagnostics will improve operation and lower costs of these accelerators and for some new multi-billion dollars facilities. The proposed electron probe tomography system with the strip cathode should be the most advanced system for detailed diagnostics of accelerated beams. It can be used in all advanced accelerators and storage rings such as EIC, SNS, Main injector FNAL, RHIC, LHC, ISIS, KEK and many others. Serial production of these diagnostics will improve operation and lower costs of these accelerators and for some new multi-billion dollars facilities.

Of particular importance to Muons, Inc. is the application of superconducting RF Linacs to drive subcritical molten-salt fueled small modular nuclear reactors to consume spent nuclear fuel (SNF) from light water reactors and advanced reactors. Our new Mu*STAR design can produce carbon-free energy for electricity generation or process heat applications while extracting almost all the energy from the SNF. After a few hundred years of storage, the remnants then have radiotoxicity that is less than uranium ore such that the nuclear fuel cycle can be closed without needing a geologic repository. The anticipated public benefits of this transformational approach to using the potential energy of the hundreds of thousands of tons of SNF that have been and will be produced by operating and future reactors include addressing climate change by providing economical electricity and by dealing with the political problems of SNF storage that have retarded the growth of nuclear energy.

The superconducting Linacs that produce the spallation neutrons needed for subcritical reactor operation will need robust, cost-effective, noninvasive tomography systems like the one that is the subject of this proposal.

Products or Technology Transfer:

Publications and Conference Papers:

V. Dudnikov, M. A. C. Cummings, G. Dudnikova, SHEET ELECTRON PROBE FOR BEAM TOMOGRAPHY, IPAC 2021, Campinas, Brazil
https://accelconf.web.cern.ch/ipac2021/papers/wepab327.pdf

Patents:
A provisional patent application for the Sheet electron Probe for Tomography is being prepared.

References

[1] Forck P. Minimal invasive beam profile monitors for high intense hadron beams. // Proc. PAC 2010, Kyoto, Japan, 2010, pp.1261-1265.

[2] V. Dudnikov, "The intense proton beam accumulation in storage ring by charge-exchange injection method," Ph.D. Thesis, Novosibirsk INP,1966;
G. Budker, G. Dimov, and V. Dudnikov, in *Proceedings of the International Symposiumon Electron and Positron Storage Rings, Saclay, France, 1966* (Saclay, Paris, 1966), Article No. VIII-6-1;(V.Dudnikov, Ph.D Thesis, INP, Novosibirsk, 1966);
G. Budker, G. Dimov, and V. Dudnikov, *Sov. Atomic. Energy* **22**, 384 (1967);
V. Dudnikov, in *Proceedings of the Particle Accelerator Conference, Chicago, 2001* (IEEE,Piscataway, NJ, 2001),

[3] Aleksandrov A., Assadi S., Cousineau S., et al. Feasibility study of using an electron beam for profile measurements in the SNS accumulator ring. // Proc. PAC 2005, Knoxville, USA, 2005, pp. 2586-2588.

[4] Roy P. K., Yu S. S., Henestroza E., et al. Electron-beam diagnostic for space-charge measurement of an ion beam. // Review of Scientific Instruments 76, 023301, 2005.

[5] Blokland W., Aleksandrov A., Cousineau S., et al. Electron scanner for SNS ring profile measurements.// Proceedings of DIPAC09, Basel, Switzerland pp.155-157. 2009.

[6] Dudnikov V., Aleksandrov A. Ribbon electron beam profile monitor for bunched beam tomography. // Proceedings of IPAC2012, New Orleans, Louisiana, USA ,2012 pp.472-474.

[7] Berezin Yu. A., Dudnikova G. I., Liseikina T. V. Fedoruk M. P. Modeling of nonstationary plasma processes, Novosibirsk: NSU, 2018 (in Russian).

[8] Vuduc R., Czechowski K. Toward a Theory of Algorithm-Architecture Co-design. In: Daydé M., Marques O., Nakajima K. (eds) High Performance Computing for Computational Science - VECPAR

[9] Glinskiy B., Kulikov I., Chernykh I., Weins D., Snytnikov A., Nenashev V., Andreev A., Egunov V., Kharkov E. The Co-design of Astrophysical Code for Massively Parallel Supercomputers, 2016.

[10] D.SatohaT.ShibuyabN.HayashizakicR.ZhangaX.ZhouaT.NatsuiaM.Yoshidaa "Research and development of iridium cerium photocathode for SuperKEKB injector linac", https://reader.elsevier.com/reader/sd/pii/S1876610217345319?token=68CF5250342D18728D1C2501D79BC67649E8120929DC1E9CE4773529A95DD4EAF9452BE141BD532911AFE9350E8FD1A2&originRegion=us-east-1&originCreation=20211120172503

"We present the results of our investigation on iridium cerium compound as a photocathode material for the SuperKEKB photoinjector. A large-size iridium cerium compound with excellent machinability was obtained by a two-stage production method combining cold crucible induction melting and spark plasma sintering, and its usability as photocathode material was verified. The quantum efficiency (QE) of the non-activated sample was measured with 266 nm laser pulses to be 2.12×10^{-6}. The QE of the cleaned sample was found to be 1.49×10^{-4}, exhibiting an improvement by a factor ~ 70. The high resistance to poisoning against oxidization and carbonization of iridium cerium compound leads to useful properties, such as the compound being easily activate by laser cleaning and its reasonably high QE being maintained under non-ultra-high vacuum conditions. These significant advantages of the iridium cerium photocathode allow for the generation of high-charge electron beams with a bunch charge of 4.8 nC, when used with an advanced radio-frequency (rf) gun in the SuperKEKB injector linac. The QE of iridium cerium compound which was mounted in the rf gun was found to stay within the range of $(8 \sim 10) \times 10^{-5}$ for a year and a half without cathode maintenance such as laser cleaning."

[11] A.A. Bashkeev, VG Dudnikov, Characteristics of microchannel plates with straight channels in saturation, Instruments and Experimental Techniques 32 (4 PT 1), 818-822 (1990).